HUMAN MUTATION 29(5), 703–708, 2008

RESEARCH ARTICLE

Integration of Hepatitis B Virus DNA Into the Myeloid/Lymphoid or Mixed-Lineage Leukemia (*MLL4*) Gene and Rearrangements of *MLL4* in Human Hepatocellular Carcinoma

Kenichi Saigo,[1,2] Kenichi Yoshida,[3]* Ryuji Ikeda,[3] Yoshiko Sakamoto,[3] Yoshiki Murakami,[4] Tetsuro Urashima,[1] Takehide Asano,[5] Takashi Kenmochi,[2] and Ituro Inoue[3,6]

[1]*Second Department of Surgery, School of Medicine, Chiba University, Chiba, Japan;* [2]*Clinical Research Center, Chiba-East National Hospital, Chiba, Japan;* [3]*Division of Genetic Diagnosis, Institute of Medical Science, University of Tokyo, Tokyo, Japan;* [4]*Center for Genomic Medicine, Kyoto University Graduate School of Medicine, Kyoto, Japan;* [5]*Hepato-Pancreato-Biliary Surgery, School of Medicine, Teikyo University, Tokyo, Japan;* [6]*Division of Molecular Life Science, School of Medicine, Tokai University, Kanagawa, Japan*

Communicated by Dr. Haig H. Kazazian, Jr.

Integration of hepatitis B virus (HBV) DNA into host DNA is detected in about 90% of HBV-related hepatocellular carcinoma (HCC), but the preferential sites of the viral integration etiologically relevant to oncogenesis have been controversial. By using an adaptor-ligation/suppression-PCR, we identified four integrations into the myeloid/lymphoid or mixed-lineage leukemia 4 (*MLL4*) gene from 10 HCC patients with positive HBV surface antigen (HBsAg). Determination of the cellular-virus DNA junction demonstrated that various lengths of the virus were integrated within 300 bp of intron 3 flanked by the Alu element of *MLL4*. Chimeric hepatitis B virus X gene (HBx)/*MLL4* transcripts and the HBx fusion proteins were detected. DNA microarray revealed that HBx/MLL4 fusion proteins suppressed unique genes in HepG2 cells. Finally, chromosomal translocations of intron 3 of *MLL4* to the specific region of chromosome 17p11.2 in 22 out of 32 HCC patients were observed, showing that the intron 3 region of *MLL4* gene would be a target of translocation breakpoint. In conclusion, the present data suggest that the translocation breakpoint of *MLL4* gene is one of the preferential targets for HBV DNA integration into the *MLL4* gene and the HBV DNA integration may be involved in liver oncogenesis. Hum Mutat 29(5), 703–708, 2008. © 2008 Wiley-Liss, Inc.

KEY WORDS: hepatocellular carcinoma; DNA integration; hepatitis B virus; HBx; *MLL4*

INTRODUCTION

Chronic human hepatitis B virus (HBV) infection causes mild to severe liver diseases, such as chronic hepatitis, liver cirrhosis, and hepatocellular carcinoma (HCC) [Block et al., 2003]. Nearly 25% of patients with chronic HBV infections terminate in untreatable liver cancer. HBV DNA frequently integrates into the human host genome, whereby insertional mutagenesis plays a crucial role in oncogenesis [Brechot et al., 2000; Gozuacik et al., 2001]. Although integration of HBV DNA is thought to be involved in oncogenesis of human hepatocytes, preferential HBV DNA integration sites targeting cellular genes were not identified until recently. Two groups have reported that HBV DNA is preferentially integrated into the human telomerase reverse transcriptase (*TERT*) gene (MIM# 187270) in HCC [Ferber et al., 2003; Paterlini-Brechot et al., 2003].

In this study, we investigated the integrated HBV DNA and flanking cellular DNA sequences. In four cases, integrations of HBV DNA into intron 3 of the myeloid/lymphoid or mixed-lineage leukemia 4 (*MLL4*) gene (MIM# 606834) were demonstrated, indicating that *MLL4* serves as a cellular target for HBV in liver oncogenesis. The *MLL4* gene is a human member of the *MLL* gene family locating on chromosome 19q13.1 [FitzGerald and Diaz, 1999], where a frequent rearrangement or amplification has been reported in solid tumors [Mitelman et al., 1997; Curtis et al., 1998]. Subsequently, we detected chromosomal translocation between intron 3 of *MLL4* and a specific region of chromosome17p11.2 in 22 HCC samples. These results indicate that intron 3 of the *MLL4* gene is one of the sites of translocation break point, which serves as a preferential target for HBV DNA integration, and may be implicated in the etiology of liver oncogenesis.

The Supplementary Material referred to in this article can be accessed at http://www.interscience.wiley.com/jpages/1059-7794/suppmat.

Received 18 September 2007; accepted revised manuscript 16 November 2007.

*Correspondence to: Kenichi Yoshida, Department of Life Sciences, Meiji University School of Agriculture, 1-1-1 Higashimita, Tama-ku, Kawasaki, Kanagawa 214-8571, Japan (present address). E-mail: yoshida@isc.meiji.ac.jp

Grant sponsor: CREST of Japan Science and Technology (II).

DOI 10.1002/humu.20701

Published online 4 March 2008 in Wiley InterScience (www.interscience.wiley.com).

PATIENTS AND METHODS

Patients

We studied 32 Japanese patients with HCC who had undergone hepatic resection without preoperative therapies at The Second Department of Surgery, Chiba University Hospital between 1987 and 2003. Serological tests for HBV were done by EIA kit (Dainabot, Tokyo, Japan) for HBV surface antigen (HBsAg), and RIA kits (Dainabot) for anti-HBs and anti-HBc antibodies. Anti-HCV antibody was tested by a recombinant immunoblot assay (Ortho Diagnostic, Westwood, MA). The study protocol conformed to the ethical guidelines of the Declaration of Helsinki (1975) and was approved by the Institutional Review Board (IRB) of Chiba University, School of Medicine. All patients gave written informed consent.

PCR and Southern Blot

HBV/cellular DNA junctions in the tumor tissues were analyzed by an adaptor-ligation/suppression-PCR [Siebert et al., 1995], according to Genomewalker Kits (Clonetech, Mountain View, CA) (Supplementary Fig. S1, available online at http://www.interscience.wiley.com/jpages/1059-7794/suppmat). Primer sequences used for PCR detection of HBV/*MLL4* and *MLL4*/HBV junctions and chromosome 19/chromosome 17 boundaries are listed in Supplementary Table S1.

Hind III-digested DNA (10 μg) were electrophoresed on 1.0% agarose gel and blotted onto nylon membrane (Hybond N+; GE Healthcare, Buckinghamshire, UK). The membrane was first hybridized with ^{32}P-labeled hepatitis B virus X gene (HBx) probe and the blot was autoradiographed. After dehybridization of the same membrane, a rehybridization was carried out with ^{32}P-labeled *MLL4* probe (the PCR products spanning exon 4 and exon 5) and autoradiographed.

RT-PCR

Total cellular RNA was extracted using Trizol (Invitrogen, Carlsbad, CA). An RT-PCR was performed with SuperScript One-Step RT-PCR system (Invitrogen) with gene-specific primers on exon 5 and exon 6 of *MLL4*. MD26c primer was used as the common sense primer. The PCR products were subjected to sequencing analyses.

Immunoprecipitation and Western Blot

Tumor tissues were lysed in a buffer containing 0.1% SDS, 0.5% deoxycholate, 1% NP-40, 150 mM NaCl, 50 mM Tris-HCl (pH 8.0), protease inhibitors (complete protease inhibitor tablets; Roche, Basel, Switzerland), and centrifuged. The supernatant was incubated with anti-HBx monoclonal antibody, generously provided by Dr. Yosef Shaul (Weizman Institute of Science), and immunoprecipitation/Western blot was performed with a standard protocol. Anti-Flag antibody was purchased from Sigma-Aldrich (St. Louis, MO).

HBx/*MLL4* Expression Plasmid, Transfection, and DNA Microarray

The HBx expression vector, pECE-X, was a gift of Dr. Jing-hsiung James Ou (University of Southern California). Human *MLL4* partial cDNA clone KIAA0304 (accession number AB002302.2) was obtained from Kazusa DNA Research Institute (Chiba, Japan). We deleted intron 7 sequence from KIAA0304 and constructed N-terminally Flag-tagged HBx/*MLL4* chimeric sequence in pcDNA3 (Invitrogen). Human hepatoma cell line HepG2 (RCB1648; RIKEN Cell Bank, Tsukuba, Japan) were transfected using Lipofectamine (Invitrogen). After 48 hr of transfection, total RNA was recovered and the microarray analysis including 12,814 unique clones from Incyte UniGene 1 was performed according to the manufacturer's instructions (Agilent Technologies, Santa Clara, CA).

RESULTS

Detection and Sequence Analysis of HBV/Cellular DNA Junctions

A total of 10 tumor specimens from HCC patients with positive HBsAg were examined for HBV DNA (accession number AB033550.1) integrations into cellular genome. The clinical backgrounds of the patients are summarized (Supplementary Table S2). We could detect four integrations into the *MLL4* gene on chromosome 19q13.1 and one into the *TERT* gene (Table 1). Integration sites of *MLL4* (accession number AD000671.1) from the four patients were all in intron 3 of the *MLL4* gene (Fig. 1A; Table 1) within or flanked with the Alu repeat sequence (Fig. 1B). As shown in Fig. 1C, full-length viral integration could be expected in HCC131 (g.17752_17753insAB033550.1:g.1827_1826), while truncated virus integrations were detected in the other three tissues, HCC143 (g.17817_17818insAB033550.1:g.2974_1794), HCC146 (g.17514_17515insAB033550.1:g.?_1807), and HCC002 (g.17542_17543insAB033550.1:g.1051_1762). In all four patients, the viral junctions described above were located in the vicinity of DR1, suggesting that the DR1 region is the preferred viral junction for HBV DNA integration.

On Southern blot analysis, clonally integrated HBV DNA sequences were detected in the tumor tissue of HCC131 and a positive control. We encountered the limitations with the heterogeneity of other samples. Using Southern blot hybridization

TABLE 1. Detection of HBV Integration and the Translocation of *MLL4* in HCC

Case no.	Chromosome	Accession no.	Gene	t(17;19)(p11;q13.1)
HCC131	19q13.1	AD000671.1	*MLL4*	Positive
HCC146	19q13.1	AD000671.1	*MLL4*	Positive
	7p14_15	AC005090.2		
HCC002	19q13.1	AD000671.1	*MLL4*	Positive
HCC003	5p13	AY007685.1	*TERT*	Positive
HCC9907	9q13_21.3	AL133578.1		Negative
HCC155				Positive
H20				Positive
H54	18p11.3	AP000845.4	*NMP p84*[a]	Positive
H120				Positive
HCC143	19q13.1	AD000671.1	*MLL4*	Positive
H49				Positive
H62				Negative
H70				Positive
H72				Positive
H78				Positive
H89				Positive
H76				Positive
H57				Negative
H71				Positive
H85				Positive
H86				Negative
H87				Positive
HCC128				Positive
HCC147				Positive
HCC127				Positive
HCC001				Positive
H148				Negative
H149				Negative
H150				Negative
HCC9833				Negative
HCC9901				Negative
HCC9906				Negative

[a]This integration was already reported. Chromosome locations, GenBank accession numbers, and gene names are indicated for eight viral/cellular junctions from seven HCC samples. Detection of t(17;19)(p11;q13.1) was indicated as positive.

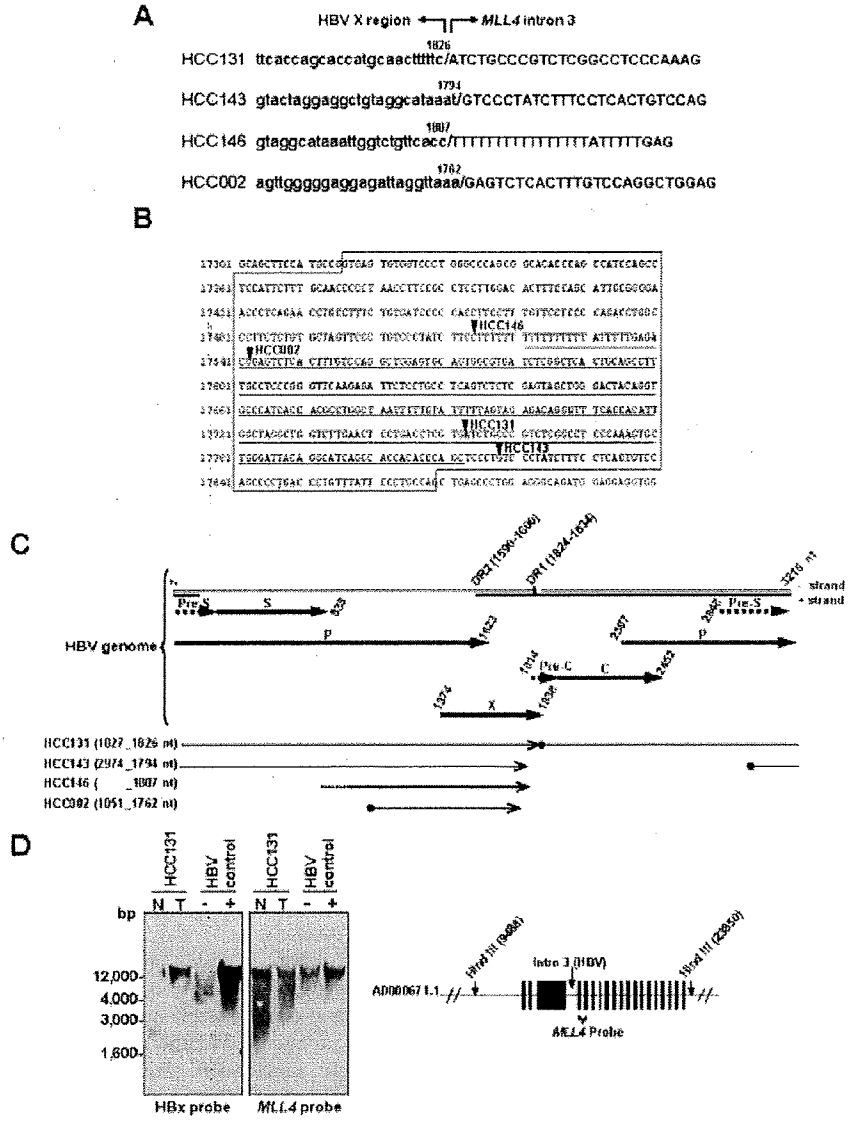

FIGURE 1. Surrounding sequences of HBV integration sites. **A:** Sequences of HBV/cellular DNA junctions in the *MLL4* gene in HCC131, HCC143, HCC146, and HCC002. In each sample, the small letters on the left show sequences of the integrated HBV DNA and capital letters on the right show the flanking *MLL4* gene sequences. Numbers above indicate HBV nucleotides at the HBV/cellular DNA junction (Accession number AB033550.1). **B:** Sequences around intron 3 of the *MLL4* gene and four HBV DNA integration sites are shown. The left side indicates nucleotide positions of *MLL4* gene (accession number AD000671.1). Intron 3 of the *MLL4* gene is indicated by the box (17316_17869 nt). The Alu repeat is shown by underline (17521_17812 nt). **C:** Schematic representation of gene organization of HBV genome and four integrated HBV genomes (HCC002, HCC131, HCC143, and HCC146). Open reading frames and their directions of transcription are represented by an arrow. The numbers above the arrow indicate location of each open reading frame (Accession number AB033550.1). DR1 and DR2 are the 11 basepair direct repeats. • and > indicate the 5′ and 3′ end of integrated HBV DNA sequences (we could not obtain the 5′ end for HCC146). The lengths of the solid lines represent the size and location of the integrated HBV. **D:** Southern blot analysis, using the HBx region as probe (left panel) and the *MLL4* probe (right panel). Hind III-digested DNAs from nontumor tissue of HCC 131 (lane 1), tumor tissue of HCC131 (lane 2), colon cancer tissue as negative control (lane 3), and the HBV integrated HCC tissue as positive control (lane 4). Schematic representation for *MLL4* gene and Hind III site are shown. HBV integration site (intron 3) and *MLL4* probe are indicated. Closed boxes indicate exons of *MLL4* gene.

with an *MLL4* probe of the same membrane, hybridization signals were also detected in the tumor tissue of the patient (Fig. 1D).

HBV Integration Into the *MLL4* Gene Drives Expression of Chimeric Transcripts

In the four HBV/*MLL4* samples, all the integrated viral genome contained HBx promoter and HBx ORF (1374_1838 nucleotides of AB033550.1) except the C-terminus (Fig. 1C). RT-PCR study for detecting fusion transcripts was carried out with HBx primer and reverse primers on various exons of *MLL4* in the four HCC tissues showing various species in each sample (Fig. 2A). In all HCC tissues, in-frame chimeric transcripts that contained exon 4 and exon 5 of *MLL4* were detected (Fig. 2B). In HCC131, two transcripts were observed; one transcript, a major form, showed in-frame fusion containing intron 3 and the other transcript retained intron 4 that led to the creation of the termination codon in exon 6. In HCC002, three transcripts were observed; one transcript

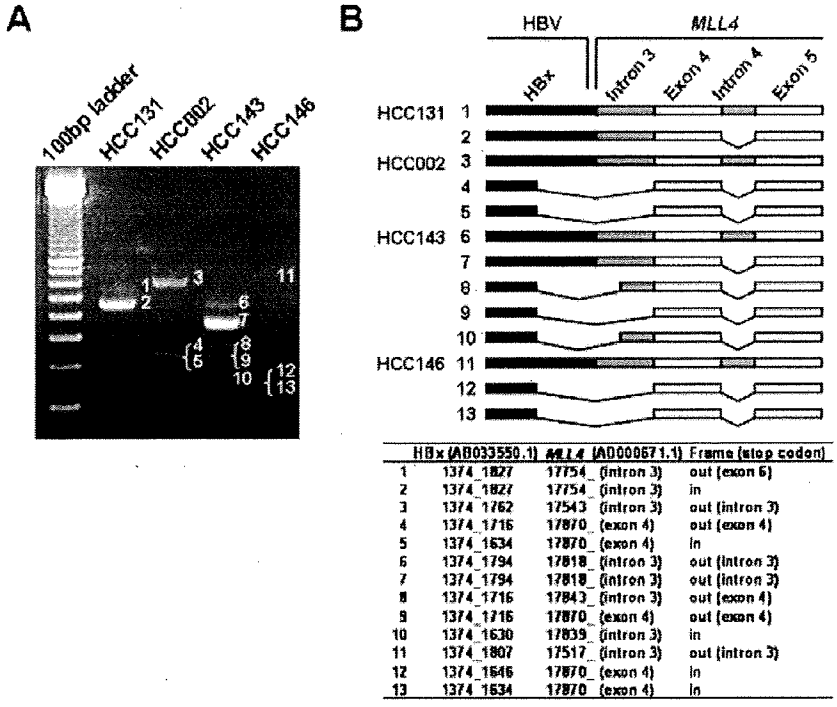

	HBx (AB033550.1)	MLL4 (AD000671.1)	Frame (stop codon)
1	1374_1827	17754_(intron 3)	out (exon 6)
2	1374_1827	17754_(intron 3)	in
3	1374_1762	17543_(intron 3)	out (intron 3)
4	1374_1716	17870_(exon 4)	out (exon 4)
5	1374_1634	17870_(exon 4)	in
6	1374_1794	17818_(intron 3)	out (intron 3)
7	1374_1794	17818_(intron 3)	out (intron 3)
8	1374_1716	17843_(intron 3)	out (exon 4)
9	1374_1716	17870_(exon 4)	out (exon 4)
10	1374_1630	17839_(intron 3)	in
11	1374_1807	17517_(intron 3)	out (intron 3)
12	1374_1646	17870_(exon 4)	in
13	1374_1634	17870_(exon 4)	in

FIGURE 2. RT-PCR analysis of HBx/*MLL4* fusion transcripts. **A:** Various transcripts were observed for each of the HCC tissues by RT-PCR. **B:** Schematic representation of the fusion transcripts from four HCC tissues (HCC131, HCC002, HCC143, and HCC146), and adjacent sequences between HBx (3′ end) and *MLL4* (5′ end) are summarized. HBx cDNA (black boxes) and *MLL4* gene (exon 4 and 5 as white boxes and intron 3 and 4 as gray boxes) are shown. Spliced out sequences are indicated by bars. Location of 5′ end of *MLL4* in intron 3 or exon 4 is also shown. Reading frame based on HBx cDNA followed by *MLL4* is indicated for individual chimeric transcripts. Location of the aberrant stop codon is also shown except for in-frame transcripts. See the Supplementary Appendix for more information.

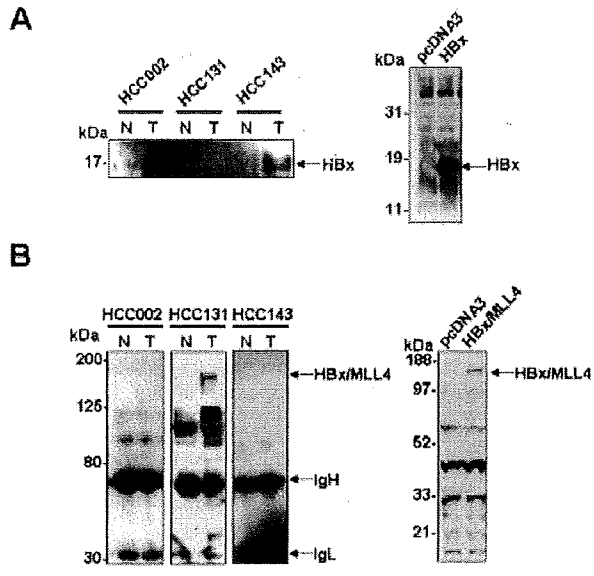

FIGURE 3. **Immunodetection of HBx fusion proteins in HCC samples. A:** Western blot analysis of tumor tissues (T) from HCC002, HCC131, and HCC143 and the adjacent nontumor tissues (N) by using the monoclonal anti-HBx antibody. Recombinant full-length HBx protein expressed in HepG2 cells are also shown. **B:** Immunoprecipitation followed by immunodetection with HBx antibody detected HBx/MLL4 putative fusion protein specifically in HCC131 T (left panel). Western blot using Flag antibody detected an approximately 170-kDa HBx/MLL4 fusion protein transiently expressed in HepG2 cells (right panel). See the Supplementary Appendix for more information.

retained intron 3 causing premature termination and the other two transcripts spliced out intron 3 using distinct 5′ splice sites, resulting in one transcript (nucleotide position 261) showing the in-frame transcript and the other (nucleotide position 343) the premature termination. Similar patterns were observed for HCC146. In HCC143, five species were observed, and the splicing junction of the in-frame transcript was CC-GT, and does not conform to the GT-AG rule.

HBx-MLL4 Fusion Proteins Expressed in HCC

To confirm that the fusion transcripts were translated, the expression of HBx-related proteins in the tumor and adjacent liver tissues were tested by immunodetection with an antibody against HBx protein. Western blot analysis showed that an approximately 17-kDa protein, which represents a short HBx fusion protein compared to recombinant full-length HBx protein expressed in HepG2 cells, is selectively expressed in the HCC002 and HCC143 tumor tissues (Fig. 3A). Immunoprecipitation followed by Western blot analysis detected an approximately 170-kDa protein in HCC131 (Fig. 3B). We constructed an expression vector that can express fusion protein consisting of N-terminally Flag-tagged HBx ORF (amino acids 1_154) and *MLL4* coding region beginning from exon 4 (corresponding to amino acids 820_2715, accession number NM_014727.1), and transiently expressed into HepG2 cells. Western blot using Flag antibody clearly detected an approximately 170-kDa protein (Fig. 3B, right panel). MLL is known to be cleaved at a conserved site and this cleavage generates N- and C-terminal fragments [Hsieh et al., 2003]. MLL4 also possesses a conserved site D/GVDD (amino acids

TABLE 2. cDNA Microarray Results Showing Upregulation and Downregulation by HBx, HBx/*MLL4* Fusion, and Truncated HBx (1_87aa) Proteins*

	Gene description	Category	HBx		HBx/MLL4		HBx1_87aa	
			Mean	SD	Mean	SD	Mean	SD
Upregulated gene name								
OR11A1	Olfactory receptor, family 11, subfamily A, member 1	G protein-coupled receptor	3.99	0.02	—		—	
OPN4	Opsin 4 (melanopsin)	G protein-coupled receptor	3.52	0.1	—		—	
UPB1	Ureidopropionase, beta	Hydrolase	3.09	0.52	—		3.89	2.2
HIST1H4L	H4 histone family, member K	Nucleosome structure	3.08	0.3	—		2.72	0.3
HIST1H4I	H4 histone family, member M	Nucleosome structure	2.8	0.02	—		—	
ELL3	Elongation factor RNA polymerase II-like 3	Transcriptional regulation	2.59	0.06	—		—	
BAI1	Brain-specific angiogenesis inhibitor 1	Cell adhesion	2.57	0.62	—		—	
CEP290	Centrosomal protein 290kDa	Centrosomal protein	2.51	0.66	—		—	
HIST1H4B	H4 histone family, member I	Nucleosome structure	2.38	0.01	—		—	
CDC2L1	Cell division cycle 2-like 1	Cell cycle	2.36	0.4	—		2.36	0.04
OR2C1	Olfactory receptor, family 2, subfamily C, member 1	G protein-coupled receptor	2.15	0.15	—		—	
DNCL2B	Dynein, light chain 2B	Motor protein	2.11	0.04	—		—	
ZNF354B	Zinc finger protein 354B	Transcriptional regulation	2.09	0.06	—		—	
MLL4	Mixed-lineage leukemia 4	Transcriptional regulation	—		31	3.25	—	
Downregulated								
AVIL	Advillin	Actin-binding protein	3	0.42	5.2	1.46	3.51	0.68
ENO2	Enolase 2	Hydratase	2.19	0.21	—		—	
KERA	Keratocan	Extracellular matrix	—		4.91	1.37	—	
UBXD1	UBX domain containing 1	Unknown	—		4.76	0.34	—	
PIAS3	Protein inhibitor of activated STAT3	Signal transduction	—		4.68	0.45	—	
MYBPC2	Fast-type myosin binding protein C	Unknown	—		4	0.48	2.48	0.12
PITPNM	Phosphatidylinositol-transfer protein membrane-associated	Cytokinesis	—		3.58	0.83	—	
EHD2	EH-domain containing 2	Endocytosis	—		3.4	0.43	—	
GJB1	Connexin 32	Gap junction	—		3.01	0.62	—	
WASL	Wiskott-Aldrich syndrome-like	Actin polymerization	—		2.48	0.22	—	
TNRC6C	Trinucleotide repeat containing 6c	Unknown	—		2.31	0.28	—	
TBC1D10B	TBC1 domain family, member 10B	Unknown	—		2.19	0.08	—	

*The experiments were performed twice, and the mean and standard deviation (SD) values were determined for each gene.

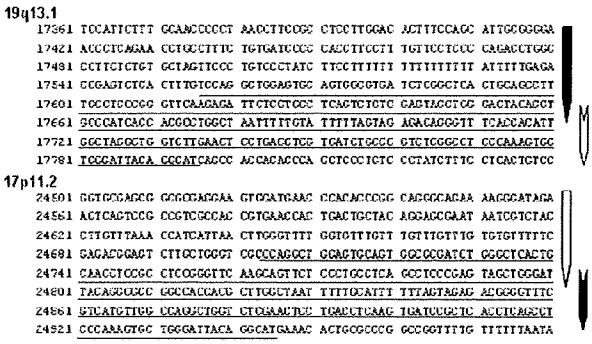

FIGURE 4. **Reciprocal translocation found in intron 3 of the *MLL4* locus. Chromosomal rearrangement between chromosome 19q13.1 (accession number AD000671.1) and chromosome 17p11.2 (accession number AC087294.18) are shown. The sequences of Alu elements are underlined. The downward pointing arrows on the respective chromosomes indicate the newly synthesized chromosomes (black-to-black and white-to-white) after the recombination events occurred via Alu elements.**

2062_2066), indicating a 170-kDa protein could be a posttranslationally modified product.

Functional Elucidation of HBx/MLL4 Fusion Protein by DNA Microarray

To provide mechanistic insights into molecular etiology such as altered target gene expression regulated by HBx/MLL4 fusion protein, we transiently overexpressed full-length HBx and HBx/MLL4 fusion proteins in HepG2 cells. We employed cDNA microarray technology and identified 13 genes that were upregulated and two genes that were downregulated by HBx protein (Table 2). In contrast, no gene (except for *MLL4* itself) was upregulated and 11 genes were downregulated by HBx/MLL4 fusion protein (Table 2). Uniquely, only one gene, Advillin (*AVIL*) was identified as a common target between HBx and HBx/MLL4 fusion proteins. We checked whether C-terminally truncated HBx protein (amino acids 1_87) could regulate the expression of genes identified by above experiments, because HBx protein in HCC002 and HCC143 only had N-terminal 87 and 86 amino acid residues. Three genes were upregulated and two genes, including *AVIL*, were downregulated by truncated HBx protein (Table 2). Taken together, these data predict that HBx/MLL4 fusion protein would suppress the expression pattern of specific genes.

Alu-Mediated Chromosomal Translocation of *MLL4* to 17p11.2 in HCC

We extended the search for HBV DNA integration into intron 3 of the *MLL4* gene in other HCC samples positive for anti-HBc antibody (Supplementary Table S2). The sequencing analyses failed to detect HBV/*MLL4* DNA sequences, instead demonstrated chimeric sequences between the *MLL4* gene and a particular region of chromosome 17p11.2 (Fig. 4). We detected 22 translocations from 32 HCC samples (Table 1). The sequencing analyses of the translocation products revealed an about 240-bp region at the junction that is highly shared by two chromosomes (approximately 85%) containing Alu elements, suggesting that Alu-mediated homologous recombination facilitated translocation (Fig. 4).

DISCUSSION

The classical mechanism by which tumor-associated viruses contribute to oncogenesis is activation of cellular genes with oncogenic potential through viral genome integration into the cellular genome. HBV genome integration into *SERCA1* (sarco/endoplasmic reticulum calcium ATPase) have been demonstrated [Chami et al., 2000]. The resultant chimeric HBx/SERCA1 protein proposed to be implicated in oncogenesis via an apoptotic

mechanism [Chami et al., 2000]. Reports from two groups, including our observation, demonstrate that the promoter region of the *TERT* gene is targeted by HBV in several HCC tissues [Ferber et al., 2003; Paterlini-Brechot et al., 2003]. Therefore, the *TERT* gene most likely serves as a nonrandom integration site of the viral genome in a subset of HBV-positive HCCs, and the oncogenic HBV DNA integrations may possess the preferential sites. In this study, we further demonstrated four cases of integrations into the *MLL4* gene in HBsAg-positive HCC samples. Sequencing analyses revealed that all of the host sites were within 300 bp of intron 3, flanked with the Alu element of the *MLL4* gene. Recently, HBV DNA integration into *MLL4* gene in three Japanese HCC patients, two cases into exon 3 integration and one into intron 3, were reported [Tamori et al., 2005]. These results support the hypothesis that the oncogenic viral integrations into hepatocytes are not entirely random.

HBV integration into intron 3 of *MLL4* resulted in several fusion transcripts between HBx and *MLL4* that could be directly implicated in liver oncogenesis, albeit the C-terminally truncated HBx protein, as observed in HCC002 and HCC143, might be more closely related to oncogenesis. Our cDNA microarray experiments indicate that HBx/MLL4 fusion protein suppressed the unique genes. It might be speculated that the fusion gene product lacking an AT hook, which is encoded in exons 1–3 of *MLL4*, is directly related to oncogenesis. Further investigation of HBx/MLL4-dependent or N-terminal MLL4-dependent transcriptional regulation may provide a novel insight into the elucidation of etiology of hepatic oncogenesis.

The *MLL4* gene, originally reported as a second human homolog of the *MLL* gene, is mapped to chromosome 19q13.1 [FitzGerald and Diaz, 1999], where gene amplification was reported in HBV-related HCCs [Marchio et al., 1997; Huntsman et al., 1999] and frequent genome rearrangements in solid tumor were reported [Curtis et al., 1998]. We detected the chromosomal translocation of the *MLL4* locus to chromosome 17 in 22 tumors out of 32 samples. The chromosomal rearrangement occurred between intron 3 of the *MLL4* gene of chromosome 19q13.1 and chromosome 17p11.2. The two chromosomal regions share nearly identical Alu elements, indicating that Alu-mediated recombination most likely explains the genome rearrangement. HBV infection and subsequent hepatitis induced DNA damage such as double-strand breaks [Dandri et al., 2002; Bill and Summers, 2004]; therefore, the genome repair mechanism is essential for maintaining the genome integrity and cellular viability.

In conclusion, we detected the translocation breakpoint point in the intron 3 of *MLL4* gene that provides one of the preferential targets for HBV integrations. Indeed we also found recurrent integrations of HBV DNA into intron 3 of *MLL4* gene in four HCC cases, and chimeric HBx/*MLL4* transcripts and HBx/MLL4 proteins, suggesting that the insertional mutagenesis could be functionally relevant to liver oncogenesis.

ACKNOWLEDGMENTS

We are grateful to Dr. Murakami (National Cancer Center Research Institute, Japan) and Dr. Miyamura, Dr. Suzuki, and Dr. Shoji (National Institute of Infectious Disease, Japan) for their technical support and helpful comments. This work was partly supported by grant from the CREST of Japan Science and Technology (II) to I.I.

REFERENCES

Bill CA, Summers J. 2004. Genomic DNA double-strand breaks are targets for hepadnaviral DNA integration. Proc Natl Acad Sci USA 101:11135–11140.

Block TM, Mehta AS, Fimmel CJ, Jordan R. 2003. Molecular viral oncology of hepatocellular carcinoma. Oncogene 22:5093–5107.

Brechot C, Gozuacik D, Murakami Y, Paterlini-Brechot P. 2000. Molecular bases for the development of hepatitis B virus (HBV)-related hepatocellular carcinoma (HCC). Semin Cancer Biol 10:211–231.

Chami M, Gozuacik D, Saigo K, Capiod T, Falson P, Lecoeur H, Urashima T, Beckmann J, Gougeon ML, Claret M, le Maire M, Brechot C, Paterlini-Brechot P. 2000. Hepatitis B virus-related insertional mutagenesis implicates SERCA1 gene in the control of apoptosis. Oncogene 19:2877–2886.

Curtis LJ, Li Y, Gerbault-Seureau M, Kuick R, Dutrillaux AM, Goubin G, Fawcett J, Cram S, Dutrillaux B, Hanash S, Muleris M. 1998. Amplification of DNA sequences from chromosome 19q13.1 in human pancreatic cell lines. Genomics 53:42–55.

Dandri M, Burda MR, Burkle A, Zuckerman DW, Will H, Rogler CE, Greten H, Petersen J. 2002. Increase in de novo HBV DNA integrations in response to oxidative DNA damage or inhibition of poly(ADP-ribosyl)ation. Hepatology 35:217–223.

Ferber MJ, Montoya DP, Yu C, Aderca I, McGee A, Thorland EC, Nagorney DM, Gostout BS, Burgart LJ, Boix L, Bruix J, McMahon BJ, Cheung TH, Chung TK, Wong YF, Smith DI, Roberts LR. 2003. Integrations of the hepatitis B virus (HBV) and human papillomavirus (HPV) into the human telomerase reverse transcriptase (hTERT) gene in liver and cervical cancers. Oncogene 22:3813–3820.

FitzGerald KT, Diaz MO. 1999. MLL2: a new mammalian member of the trx/MLL family of genes. Genomics 59:187–192.

Gozuacik D, Murakami Y, Saigo K, Chami M, Mugnier C, Lagorce D, Okanoue T, Urashima T, Brechot C, Paterlini-Brechot P. 2001. Identification of human cancer-related genes by naturally occurring hepatitis B virus DNA tagging. Oncogene 20:6233–6240.

Hsieh JJ, Ernst P, Erdjument-Bromage H, Tempst P, Korsmeyer SJ. 2003. Proteolytic cleavage of MLL generates a complex of N- and C-terminal fragments that confers protein stability and subnuclear localization. Mol Cell Biol 23:186–194.

Huntsman DG, Chin SF, Muleris M, Batley SJ, Collins VP, Wiedemann LM, Aparicio S, Caldas C. 1999. MLL2, the second human homolog of the Drosophila trithorax gene, maps to 19q13.1 and is amplified in solid tumor cell lines. Oncogene 18:7975–7984.

Marchio A, Meddeb M, Pineau P, Danglot G, Tiollais P, Bernheim A, Dejean A. 1997. Recurrent chromosomal abnormalities in hepatocellular carcinoma detected by comparative genomic hybridization. Genes Chromosomes Cancer 18:59–65.

Mitelman F, Mertens F, Johansson B. 1997. A breakpoint map of recurrent chromosomal rearrangements in human neoplasia. Nat Genet 15:417–474.

Paterlini-Brechot P, Saigo K, Murakami Y, Chami M, Gozuacik D, Mugnier C, Lagorce D, Brechot C. 2003. Hepatitis B virus-related insertional mutagenesis occurs frequently in human liver cancers and recurrently targets human telomerase gene. Oncogene 22:3911–3916.

Siebert PD, Chenchik A, Kellogg DE, Lukyanov KA, Lukyanov SA. 1995. An improved PCR method for walking in uncloned genomic DNA. Nucleic Acids Res 23:1087–1088.

Tamori A, Yamanishi Y, Kawashima S, Enomoto M, Tanaka H, Kudo S, Shiomi S, Nishiguchi S. 2005. Alteration of gene expression in human hepatocellular carcinoma with integrated hepatitis B virus DNA. Clin Cancer Res 11:5821–5826.

Available online at www.sciencedirect.com
ScienceDirect
Virology 375 (2008) 424–432
VIROLOGY
www.elsevier.com/locate/yviro

Isolation and gene analysis of interferon α-resistant cell clones of the hepatitis C virus subgenome

Tohru Noguchi [a,b,*], Tomoko Otsubaki [a], Izuru Ando [a], Naoki Ogura [a], Satoru Ikeda [a], Kunitada Shimotohno [b,1]

[a] *Central Pharmaceutical Research Institute, Japan Tobacco Inc., Takatsuki, Osaka 569-1125, Japan*
[b] *Laboratory of Human Tumor Viruses, Department of Viral Oncology, Institute for Virus Research, Kyoto University, Kyoto, Kyoto 606-8507, Japan*

Received 5 November 2007; returned to author for revision 27 November 2007; accepted 10 February 2008
Available online 18 March 2008

Abstract

Hepatitis C virus (HCV) proteins appear to play an important role in IFN-resistance, but the molecular mechanism remains unclear. To clarify the mechanism in HCV replicon RNA harboring Huh-7 cells (Huh-9-13), we isolated cellular clones with impaired IFNα-sensitivity. Huh-9-13 was cultured for approximately 2 months in the presence of IFNα, and 4 IFNα-resistant cell clones showing significant resistances were obtained. When total RNA from clones was introduced into Huh-7 cells, the transfected cells also exhibited IFNα-resistance. Although no common mutations were present, mutations in NS3 and NS5A regions were accumulated. Transactivation of IFNα and IFNα-stimulated Stat-1 phosphorylation were reduced, and the elimination of HCV replicon RNA from the clones restored the IFNα signaling. These results suggest that the mutations in the HCV replicon RNA, at least in part, cause an inhibition of IFN signaling and are important for acquisition of IFNα resistance in Huh-9-13.

Keywords: Hepatitis C virus; Replicon; Interferon resistance; Stat-1; Nonstructural protein NS5A

Introduction

Hepatitis C virus (HCV) is the major cause of post-transfusion non-A non-B hepatitis. Approximately 170 million individuals worldwide were estimated to be infected with HCV (Alter, 1997). It has been suggested that the development of liver cirrhosis and hepatocellular carcinoma are consequences of chronic infection with HCV (Hijikata et al., 1993b; Tong et al., 1995).

HCV, a member of the *Flaviviridae* family, has a single-stranded positive-sense linear RNA genome of about 9.5 kb (Hijikata et al., 1991; Kato et al., 1990; Takamizawa et al., 1991). The RNA encodes a single precursor polyprotein of approximately 3010 amino acids (Choo et al., 1991; Okamoto et al., 1991, 1992) that is co- and post-translationally cleaved to produce individual structural (Core, E1, E2) and nonstructural proteins (NS2, NS3, NS4A, NS4B, NS5A, and NS5B) by both host and viral proteases (Hijikata et al., 1993a,b; Houghton, 1996).

The cell line Huh-9-13, in which the HCV subgenome can self-replicate, was established by R. Bartenschlager's group (Lohmann et al., 1999). The HCV subgenomic RNA consists of the entire nonstructural coding region of the Con1 strain of the HCV genome, except for the neomycin-resistant gene. This cell line provides significant information for understanding the replication of the HCV genome and is useful as a powerful screening tool for developing anti-HCV drugs (Bartenschlager et al., 2000, 2001).

Interferon alpha (IFNα) is widely used for the treatment of patients with chronic HCV infection; however, the effectiveness of IFNα, especially in genotype 1b, is low at only about 20–30% (Lindsay, 1997), although combination therapy with Ribavirin improves treatment outcomes (up to 50–60%) (McHutchison et al., 1998). According to reports of epidemiologic analysis conducted in Japan, IFN treatment outcomes are related with mutations within a 40 amino acid sequence in NS5A (amino acid

* Corresponding author. Central Pharmaceutical Research Institute, Japan Tobacco Inc., Takatsuki, Osaka 569-1125, Japan. Fax: +81 726 81 9783.
E-mail address: toru.noguchi@ims.jti.co.jp (T. Noguchi).
[1] Current address: Center for Integrated Medical Research, Keio University, Tokyo, Shinjuku 160-8582, Japan.

0042-6822/$ - see front matter © 2008 Elsevier Inc. All rights reserved.
doi:10.1016/j.virol.2008.02.009

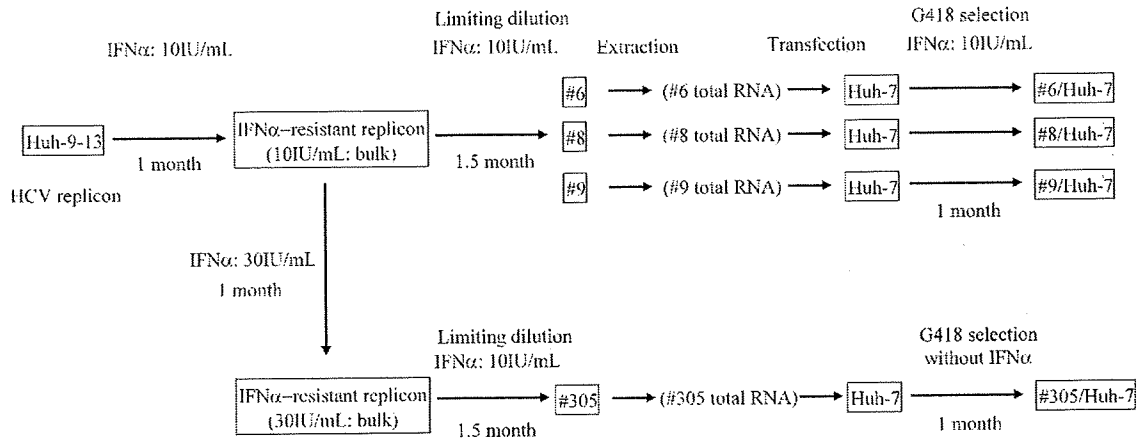

Fig. 1. An outline of the process used for isolation of replicon cells showing IFNα-resistance. Total RNA transfection derived from replicons to naive Huh-7 cells was performed using DMRIE-C reagent (Invitrogen).

(A)

	Cell	EC50(IU/mL)	Fold reduction
Original	Huh-9-13	0.7	1.0
IFNα–resistant	#6	6.9	9.5
	#8	6.7	9.2
	#9	10.2	13.9
	#305	99.2	135.6

(B)

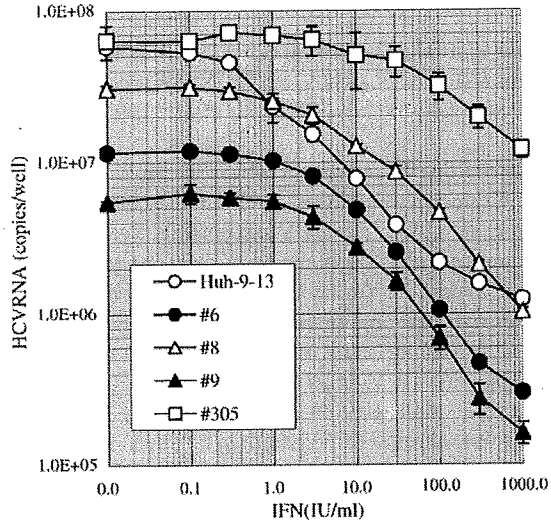

Fig. 2. Reactivity for IFNα in established IFNα-resistant replicon cells (#6, #8, #9, and #305) and original replicon cells (Huh-9-13). The cells were treated with IFNα for 48 h, and the amount of HCV RNA was measured by quantitative RT-PCR. (A) EC_{50} value (IU/mL) of IFNα in each replicon and fold reduction of the value compared to original replicon (Huh-9-13). (B) Change in copy number of HCV RNA in original and IFNα-resistant replicons by IFNα treatment. These experiments were performed in triplicate and mean values are shown.

numbers 2209–2248, based on the sequence of the prototype for HCV-J polyprotein) called the interferon sensitivity determining region (ISDR) (Enomoto et al., 1996). However, it is not clear how NS5A functionally interacts with IFN signals. Alternatively, NS5A is shown to inhibit the activity of double-stranded RNA (dsRNA)-activated protein kinase (PKR) and 2′-5′-oligoadenylate synthetase (2′-5′-OAS) induced by IFNα (Gale et al., 1997; Noguchi et al., 2001; Taguchi et al., 2004).

Recently, Meylan et al. and other groups reported that HCV-NS3-4A protease cleaved Cardif (Meylan et al., 2005) (also designated as VISA (Xu et al., 2005), MAVS (Seth et al., 2005), IPS-1 (Kawai et al., 2005)) and suppressed IFN production through RIG-I signaling. Cardif interacts with RIG-I (Yoneyama et al., 2004) mediated through CARD domains in both molecules

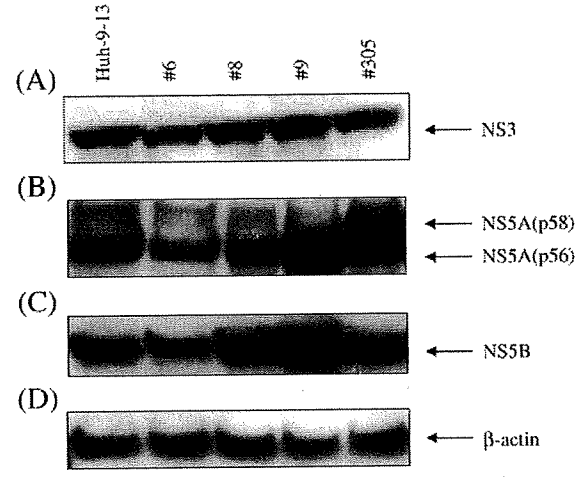

Fig. 3. Western blot analysis of the established IFNα-resistant replicon cells (#6, #8, #9, and #305) and original replicon cells (Huh-9-13). Expression of β-actin was used as an internal control of cellular protein in the replicon cells. Each cell line was inoculated on a 60-mm plate at 3×10^5 cells/well. Twenty-four hours after inoculation, the cells were lysed with SDS sample buffer. Total proteins were subjected to a 2/15% SDS gradient gel, and were subsequently immunoblotted by NS3 (A), NS5A (B), NS5B (C), and β-actin (D) antibody.

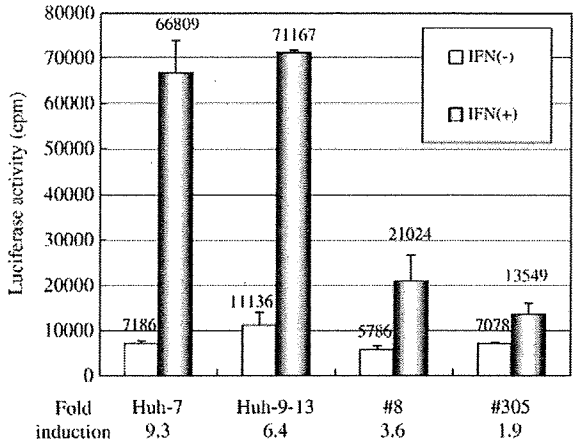

Fig. 4. Transactivation of ISRE in IFNα-resistant replicon cell lines (#8 and #305), original replicon (Huh-9-13), and parental Huh-7 cells by reporter gene (pISRE/Luc) analysis. The cells were stimulated with 1000 IU/mL of IFNα for 24 h after transfection of reporter plasmid DNA. White bars show control (no addition of IFNα) luciferase activity, and black bars show the activity under IFNα stimulation. Values of luciferase activity by IFNα stimulation relative to those of untreated cells are shown below the panel as 'fold induction'.

in a dsRNA-dependent manner, and transduce IFN production signals through the activation of nuclear factor κB (NFκB) and interferon regulatory factor 3 (IRF-3).

Despite bearing an HCV-1b genotype-derived replicon with mutations in ISDR, the replicon cells do not show resistances to IFN (Frese et al., 2002; Guo et al., 2001, 2004). Concerning this point, some reports regarding IFN-resistance acquisition and analysis of this property in the replicon cells (Namba et al., 2004; Sumpter et al., 2004; Zhu et al., 2005) showed involvement of various factors such as viral and/or host gene alterations participating in IFNα-resistance in replicon cells.

Here, we isolated IFNα-resistant clones of the HCV subgenome with accumulated mutations, especially in NS3 and NS5A regions. We observed impairment of phosphorylation of Stat-1 in cells bearing the IFNα-resistant HCV replicon. Our findings suggest that NS5A contributes to the acquisition of IFNα-resistant phenotype in HCV replicon cells.

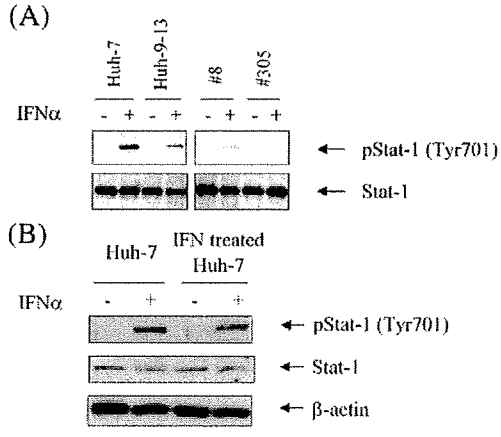

Fig. 5. (A) Change in phosphorylation of Stat-1 in IFNα-resistant replicon cell lines (#8 and #305), original replicon (Huh-9-13) and parental Huh-7 cell. Phosphorylation of Stat-1 was analyzed by western blot analysis using anti-phospho-Stat-1 (Tyr701) antibody. The cells were cultured in medium with or without 500 IU/mL of IFNα for 30 min. Upper panel represents a phospho-Stat-1 (Tyr701) and lower panel shows a Stat-1. Western blot analysis was performed as described in Materials and methods. (B) Change in phosphorylation of Stat-1 in Huh-7 cells maintained in the presence or absence of IFNα (10 IU/mL) for 4 weeks. Upper panel represents a phospho-Stat-1 (Tyr701), middle panel shows a Stat-1 and lower panel shows a β-actin. Phosphorylation of Stat-1 in these cells was examined as described above.

Results

Establishment of IFNα-resistant replicon cell lines

HCV replicon cells were cultured for approximately 1 month in the presence of 10 IU/mL IFNα. HCV RNA titer decreased during the culture; however, the appearance of cells less sensitive to IFNα during prolonged culture was observed by quantitative RT-PCR. The resistant cells were then cloned by limiting dilution. Three clones (Fig. 1: #6, #8, and #9) were obtained, and mixed pools of these resistant cells were further selected in the presence of 30 IU/mL IFNα for another 4 weeks. After confirming decreased sensitivity to IFNα at this dose, the clone

(A)

	Cell	IFN selection	EC50 (IU/mL)	Fold Reduction
Total RNA transfection	Huh-9-13/Huh-7	(-)	0.7	1.0
	#305/Huh-7	(-)	4.1	5.9
original	Huh-9-13	(-)	0.6	1.2

(B)

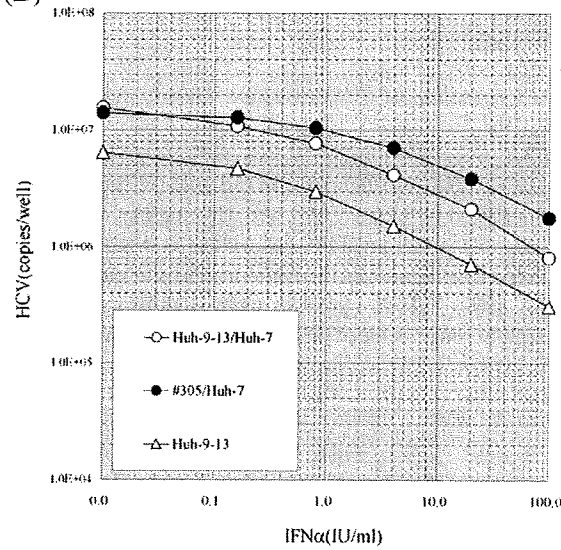

Fig. 6. Reactivity for IFNα in the Huh-7 cells, #305/Huh-7, transfected with total RNA of #305 replicon cells and in the Huh-7 cells, Huh-9-13/Huh-7, transfected with total RNA of original replicon cells (Huh-9-13). These transfected cells were selected with G418 in the absence of IFNα. The amount of HCV RNA was analyzed by quantitative RT-PCR, as described in Fig. 2. (A) EC_{50} value (IU/mL) of IFNα in Huh-9-13/Huh-7 and #305/Huh-7. (B) Change in copy number of HCV RNA in Huh-9-13/Huh-7 and #305/Huh-7 by IFNα treatment. These experiments were performed in triplicate and mean values are shown.

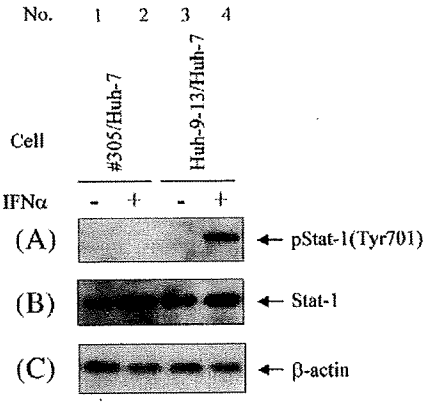

Fig. 7. Phosphorylation of Stat-1 in #305/Huh-7 and Huh-9-13/Huh-7 described in Fig. 6. The experiment was performed as described in Fig. 5. Each panel shows (A) phospho-Stat-1 (Tyr701), (B) Stat-1, and (C) β-actin. (Lanes 1 and 2) Huh-7 cells transfected with IFNα-resistant replicon (#305) total RNA (#305/Huh-7). (Lanes 3 and 4) Huh-7 cells transfected with original replicon (Huh-9-13) total RNA (Huh-9-13/Huh-7).

(Fig. 1; #305) showing highest resistance to IFNα was obtained. Sensitivities of these clones to IFNα are shown in Fig. 2. The basal HCV RNA levels in these cells (#6, #8, #9, and #305) were almost equal to that in the original replicon cells (Huh-9-13). The EC_{50} value of IFNα for the original replicon (Huh-9-13) was 0.7 IU/mL, compared to 6.9 IU/mL, 6.7 IU/mL, 10.2 IU/mL, and 99.2 IU/mL for resistant clones #6, #8, #9, and #305, respectively. These results demonstrate that sensitivity to IFNα based on EC_{50} value decreased 9 to 135-fold in the IFNα-resistant clones.

Characterization of IFNα-resistant replicon cell lines

First, expression of HCV NS proteins (NS3, NS5A, and NS5B) in IFNα-resistant replicon cell lines (#6, #8, #9, and #305) was analyzed by western blot. We detected expression of all the NS proteins in these cell lines as well as in original replicon cell (Huh-9-13) at almost at the same levels, although the levels of NS5A and NS5B in clone #6 were slightly low (Fig. 3). Interestingly, only clone #305 exhibited a different migration of NS5A, corresponding to the size of hyper-phosphorylated form (p58) in addition to the size of basal phosphorylated form (p56).

To analyze the change in IFNα signal transduction in two representative IFNα-resistant replicon cell lines (#8 and #305), we carried out a reporter gene assay using a firefly luciferase gene fused with three repeats of an ISG15-type IFN-stimulated responsive element (ISRE) as a reporter construct (pISRE/Luc). After transfection of pISRE/Luc to these replicon cells, the cells were stimulated with 1000 IU/mL of IFNα for 24 h. As shown in Fig. 4, the transactivation by IFNα in original replicon cells (Huh-9-13) was slightly reduced compared with that of parental cell line Huh-7 (Huh-7, 9.3-fold; Huh-9-13, 6.4-fold). Luciferase activity of #8 and #305 was more diminished than that of Huh-9-13 (#8, 3.6-fold; #305, 1.9-fold). The extent of decline of transactivation by IFNα treatment in these resistant replicon cell lines was dependent on the extent of IFNα-resistance, as quantified by RT-PCR (Fig. 2). It is suggested that the genetic alteration in HCV replicon RNA confers on IFNα-resistance in these cell lines.

In relation to the reporter gene analysis, JAK-STAT pathway activated by type I IFN was analyzed in IFNα-resistant replicons containing cells (#8 and #305). Phosphorylation of Stat-1, one of the important molecules in the JAK-STAT signal transduction pathway, was lowered in original replicon cells (Huh-9-13) compared with that in parental Huh-7 (Fig. 5A). However, severely impaired phosphorylation of Stat-1 was observed in the IFNα-resistant replicons containing cells (#8 and #305) compared with original replicon cells (Huh-9-13) (Fig. 5A). Furthermore, phosphorylation of Stat-1 was also decreased in #305 containing cells maintained in the absence of IFNα for 4 weeks, and the degree of decrease of Stat-1 phosphorylation was almost equal to that maintained in the presence of IFNα (data not shown). In contrast to these observations, Huh-7 cells, the parental cell of Huh-9-13 that was maintained in the presence of IFNα for 4 weeks did not show the significant alteration of Stat-1 phosphorylation compared with that maintained in the absence of IFNα (Fig. 5B). These results suggest that reduction of phosphorylation of Stat-1 in these IFNα-resistant replicon cell lines is caused by alteration of HCV replicon RNA and it may correlate with suppression of transcription from the reporter gene (Fig. 4).

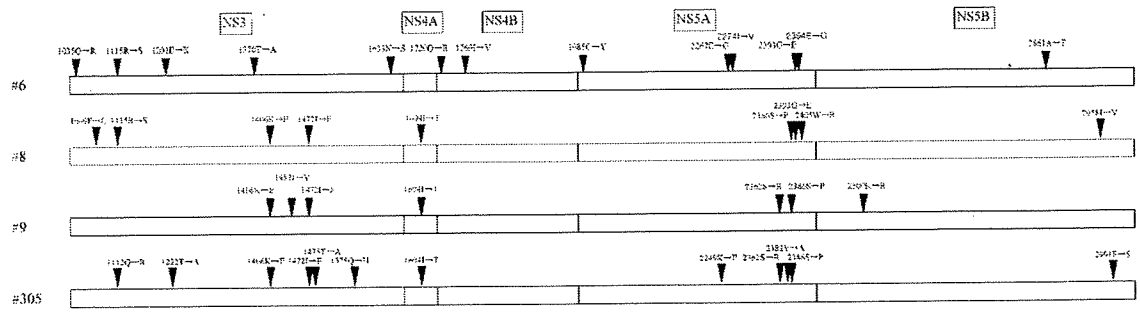

Fig. 8. The amino acid sequence deduced from nucleotide sequence in IFNα-resistant replicon cells. The nucleotide sequence was determined by an RT-PCR direct sequencing method. Arrows indicate the amino acid substitutions that were detected only in IFNα-resistant replicons compared with original replicon (Huh-9-13). The numbering of amino acids was referred to that of complete polyprotein of the isolate.

HCV replicon RNA confers IFNα-resistance

To confirm the role of HCV subgenomic RNA from clone #305 for acquisition of IFNα-resistance, total RNA was extracted from the cells and transfected to naive Huh-7 cells. The transfected cells were selected with G418 in the absence of IFNα. HCV negative-stranded replicon RNA, replication intermediate, and HCV NS proteins (NS3, NS5A and NS5B) were detected in the cells (data not shown).

Concerning the cells transfected with total RNA from IFNα-resistant #305 cell (#305/Huh-7) or the cells transfected with total RNA from original Huh-9-13 replicon cell (Huh-9-13/Huh-7), IFNα-sensitivity (EC_{50}) was analyzed (Fig. 6). IFNα-sensitivity (EC_{50}) of the Huh-9-13/Huh-7 showed 0.7 IU/mL, whereas the #305/Huh-7 showed 4.1 IU/mL. EC_{50} values of the Huh-7 cells bearing IFNα-resistant replicon derived from clone #305 were approximately 6-fold higher than that of Huh-7 cells bearing the original replicon. Although IFNα-resistance (EC_{50}) of the cells bearing #305 RNA was not as high as that of original #305, this finding suggests that acquisition of IFNα-resistance of these cells was due to genetic alteration of the replicon RNA.

We investigated the phosphorylation status of Stat-1 by stimulation of IFNα in these cells. As shown in Fig. 7, phosphorylation of Stat-1 in #305/Huh-7 (lane 2) was suppressed compared with that in Huh-9-13/Huh-7 (lane 4), suggesting that the IFNα-resistant HCV replicon derived from #305 is responsible for acquisition of the decreasing response to Stat-1 phosphorylation stimulated by IFNα.

Direct sequencing analysis of IFNα-resistant replicons

Nucleotide sequences in the NS region of each resistant clone were determined by RT-PCR direct sequencing. Sites of mutation that were detected only in IFNα-resistant replicons are shown by arrowheads and numbers (N-terminus of NS3 was denoted as 1027 based on the numbering of the complete polyprotein of the isolate), together with conversion of amino acids by arrows (Fig. 8). Although synonymous mutations are clustered in NS3 and the C-terminal region of NS5A, there were no common mutations among these resistant clones. Moreover, no mutations located at the positions as in IFNα-resistant replicons established by Namba et al. (2004) and Sumpter et al. (2004) were found in the present study. Mutations in the ISDR of NS5A were reported

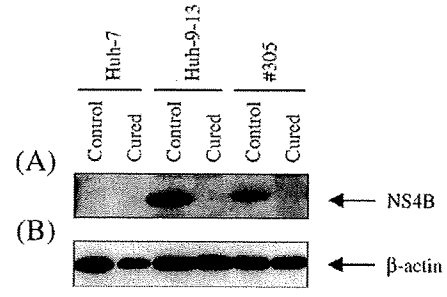

Fig. 9. Expression of NS protein (NS4B) (A) and β-actin (B) was confirmed in 'cured cells' by western blot analysis. Huh-7 cells with JTP-71892 as well as replicon cells (Huh-9-13 and #305) were analyzed likewise.

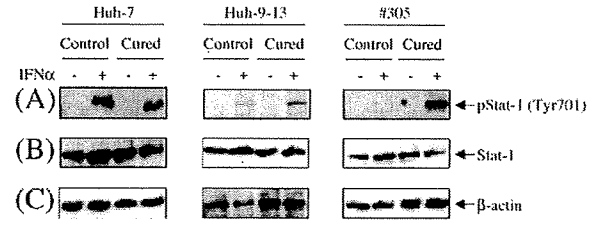

Fig. 10. Phosphorylation of Stat-1 (Tyr701) in 'cured cells'. Phosphorylation of Stat-1 (Tyr701) (A) by IFNα stimulation was investigated by western blot analysis. Stat-1 (B) and β-actin (C) were also analyzed. IFNα stimulation and western blot analysis were performed as described in Fig. 5.

to play an important role in outcome of IFN treatment to patients with genotype 1b of HCV in Japan (Enomoto et al., 1996); however, the amino acid sequence of ISDR was preserved among these replicon cell lines in our experiments.

Characterization of 'cured cells' obtained by IFNα-resistant HCV replicon cells

To clarify the role of HCV replicon RNA in resistance to IFNα, the replicon cells (Huh-9-13 and #305) were treated with JTP-71892 (1 μM) for more than 1 month to establish 'cured cells', as described in Materials and methods. JTP-71892 is a JTK-109-derivative synthesized in our laboratory, which has a potent inhibitory effect on HCV replication (Hirashima et al., 2006). The amounts of HCV replicon RNA in both replicon-bearing cell types were decreased less than what could be detected by quantitative RT-PCR, while the amounts of GAPDH mRNA used as a control did not show any difference (data not shown). The representative HCV NS protein, NS4B, was not detected in the 'cured cells' (Fig. 9).

The phosphorylation status of Stat-1 was then analyzed in these cells. The Stat-1 phosphorylation (Tyr701) by IFNα stimulation has restored remarkably in 'cured cells' (derived from both Huh-9-13 and #305) (Fig. 10). There was no obvious difference in the extent of Stat-1 phosphorylation by JTP-71892 treatment in Huh-7, indicating that restoration of Stat-1 phosphorylation was not due to JTP-71892. There was no clear difference in the amount of non-phosphorylated Stat-1 and β-actin expression by the IFNα stimulation or JTP-71892 treatment among these cell clones. These results suggest that HCV replicon RNA contributes to IFNα-resistance through impairment of phosphorylation of Stat-1, at least in part.

Discussion

We cultured HCV replicon cells in the presence of 10 and 30 IU/mL IFNα to isolate IFNα-resistant clones. Four different resistant clones with differing sensitivities to IFNα were isolated. The sensitivity for IFNα attenuated more than 100-fold in the #305 replicon, which was isolated in the presence of 30 IU/mL of IFNα and showed the most remarkable resistance in our study.

We analyzed the appearance of G418-resistant cells, #305/Huh-7, obtained by transfection of total RNA from the IFNα-

resistant replicon-bearing cells to Huh-7 by culturing them in the absence of IFNα, as shown in Fig. 1. IFNα sensitivities of the Huh-7 cells transduced with HCV replicon RNA of #305 cells were about 6-fold lower than those transfected with total RNA of original replicon cells (Huh-9-13), in coincident with a reduction of Stat-1 phosphorylation. However, #305/Huh-7 conferred a lesser extent of IFNα-resistance compared with that of parental #305 (Figs. 2 and 6). Although some factors other than HCV replicon RNA itself may participate in acquisition of IFNα-resistance in #305 cells, these results suggest that replicon RNA derived from #305 was significantly involved in regulation of IFNα signaling. The 'cured cells', from which HCV genomic RNA was removed from IFNα-resistant replicon cell line (#305) after treatment with 1 μM of JTP-71892, a potent HCV replication inhibitor, resulted in restoration of IFNα signaling to parental Huh-7. This finding suggests that HCV replicon RNA plays important roles in suppression of Stat-1 function. Moreover, this effect is dependent on mutation of HCV replicon RNA.

Mutations of amino acids were clustered throughout the whole region of NS3 and the C-terminus of NS5A in the IFNα-resistant replicon RNAs; however, there were no common amino acid mutations among the clones. This result may suggest the possibility that a change of plural functions participates in the acquisition of resistance. Whereas we did not identify common mutations, four amino acid mutations, K1406E, I1472F, I1694T, and S2386P, in NS3/4A and NS5A were shown to be common in #8, #9, and #305. In particular, the mutation at S2386P in NS5A located near region V3, one of the important prediction factors of the outcome in clinical IFN therapy (Nousbaum et al., 2000; Puig-Basagoiti et al., 2005), is found in #9 and #305. The nucleotide sequence of ISDR region was preserved between original replicon and IFNα-resistant replicons.

Concerning the mutations in NS5A region of #305, we established 3 chimeric replicon cell clones harboring Huh-9-13 replicon that was substituted with NS5A coding region derived from #305, which was selected by G418 in the absence of IFNα. These cell clones showed reduction of IFNα sensitivity (EC_{50}) as 20 to 30 times as those of normal replicon cell (Huh-9-13). Although chimeric replicons harboring #305 NS5A showed lesser extent of IFNα-resistance than that of #305 replicon cell, NS5A of #305 plays an important role in acquisition of IFNα-resistance in the replicon cell (data not shown).

Naka et al. (2005) reported that nonsense mutations and deletions of type I IFN receptor genes (IFNAR1, IFNAR2c) were found in certain clones of replicon cells that gained IFNα-resistance. However, we did not detect any such mutation or deletion in either of these genes in this work. Furthermore, we were not able to obtain resistant phenotype by IFN treatment at high concentrations of more than 1000 IU/mL.

In #305, among other IFNα-resistant clones, substantial amount of slow migrating form of NS5A was observed. From previous reports (Asabe et al., 1997, Ide et al., 1997; Kaneko et al., 1994; Kim et al., 1999; Reed et al., 1997, 1998; Tanji et al., 1995), it is supposed that this form is hyper-phosphorylated NS5A with 58 KD. Hyper-phosphorylated form of NS5A (p58) negatively participates in replication of HCV RNA in replicon cells (Appel et al., 2005; Evans et al., 2004; Huang et al., 2006; Neddermann et al., 2004). However, the quantity of basal HCV replication in #305 was almost the same as in other replicon cells, including Huh-9-13. Thus, it is likely that the hyper-phosphorylation of NS5A does not contribute to suppression of replication of HCV replicon. Rather, it may be related to a potent IFNα-resistance in #305 via un-identified mechanisms. Further studies are needed to clarify the role of hyper-phosphorylated NS5A in IFNα-resistance.

Concerning effects of NS5A on IFN signaling, it was reported that transiently- or stably-transfected NS5A inhibits IFN-stimulated Stat-1 phosphorylation and transactivation of ISRE in hepatocyte-derived cell lines, including Huh-7 cell (Gong et al., 2007; Lan et al., 2007). These authors also suggested the interaction of NS5A with Stat-1. Although these evaluation methods were different from that of our replicon system, they lend additional credibility to the suggestion that NS5A plays an important role in regulation of IFN signaling via inhibition of Stat-1 phosphorylation.

Stat-1 phosphorylation by IFNα stimulation was suppressed in IFNα-resistant replicon cells. The degree of suppression of Stat-1 phosphorylation was related to the sensitivity of IFNα in IFNα-resistant replicons (Fig. 5A). Moreover, the decrease of Stat-1 phosphorylation in #305 cells maintained in the absence of IFNα for 4 weeks was almost same level as that maintained in the presence of IFNα, suggesting that IFNα pressure did not induce a negative feedback (i.e. leading to the degradation of IFN receptor) loop in our experimental system. In contrast, Stat-1 phosphorylation was not changed significantly in parental Huh-7 cells that were maintained in the presence of IFNα compared with that maintained in the absence of IFNα (Fig. 5B), suggesting that Stat-1 phosphorylation in the parental Huh-7 cells was not affected with IFNα pressure and that the alteration of HCV replicon confers the IFNα-resistance. Stat-1 phosphorylation was also suppressed in the Huh-7 cells transfected with total RNA from IFNα-resistant replicon (Fig. 7). Moreover, the 'cured cells' showed a restoration of Stat-1 phosphorylation (Fig. 10). These observations suggest that IFNα-resistance in IFNα-resistant replicon cells depends on a change in Stat-1 phosphorylation, at least in part. For unknown reasons, we could not detect phosphorylation of Stat-2 (Tyr689), Stat-3 (Tyr705) (Sarcar et al., 2004; Zhu et al., 2005), JAK-1 (Tyr1022), or Tyk-2 (Tyr1054) in these cells. Concerning these proteins in the replicon cells, further investigation is needed to understand their roles in acquisition of IFNα-resistance.

Although the underlying mechanism of acquisition of IFNα-resistance gained by HCV replicon RNA remains unclear, clarification of detailed analysis of the role of Stat-1 in regard to IFN signaling in HCV replicon cells may contribute to the development therapeutic agents.

Materials and methods

Cell culture

Huh-9-13 cells harboring HCV subgenomic (NS3-3′X) replicon and parental Huh-7 cells were purchased from ReBLikon GmbH. Cells were cultured in Dulbecco's modified Eagle's

medium (DMEM) supplemented with 10% fetal bovine serum. To Huh-9-13 cells, 1 mg/mL of G418 (Geneticin; Invitrogen), a selective marker for replicated HCV subgenome was added.

IFN treatment

Huh-9-13 cells were seeded in a 75-cm^2 flask at a density of 3×10^5 cells/flask. Twenty-four hours after cell seeding, human IFNα (Sumiferon®300; Dainippon Sumitomo Pharma) was added so that the final concentration in medium was 10 IU/mL. Control cells were cultured in medium with no other additional substances. Cell passages were performed approximately every 7 days and the cells were cultured for approximately 1 month in the presence of IFNα (10 IU/mL). After decreases in sensitivity to IFNα were confirmed in the IFNα-treated groups by quantitative RT-PCR, IFNα-resistant cell phenotypes were further cultured for about 1 month in the presence of 30 IU/mL IFNα, and sensitivity to IFNα was then also measured in these cells. The cells cultured in the presence of 10 or 30 IU/mL of IFNα were cloned by a limiting dilution method using 96-well plates: cells were seeded at 1 cell/well and cultured in medium containing 10 IU/mL IFNα. After culture for about two to three weeks, survival and growth of cloned cells were confirmed, and then colonies were isolated and added to 48-well plates containing the test substance in 500 μL of culture medium per well. The proliferated cells in the 48-well plates were transferred to 6-well plates, and these were further put into 75-cm^2 cell culture flasks for subculture. Thereafter, subculture passage was performed approximately every 7 days. Cloning and subculture were performed in the presence of IFNα.

Measurement of IFN-sensitivity (quantitative analysis of HCV replicon and GAPDH mRNA)

IFN-sensitivity of IFNα-treated replicon cells was measured by quantitative RT-PCR. Cells (1×10^4 cells/well) were seeded in 96-well plates in the presence of 0, 0.1, 0.3, 1, 3, 10, 30, 100, 300, or 1000 IU/mL of IFNα. Forty-eight hours after cultivation with IFNα, the cells were harvested to extract total RNA using a total RNA extraction kit (RNeasy® 96; Qiagen) in accordance with the instruction manual. Quantification of HCV replicon RNA in the prepared RNA was performed using TaqMan® EZ RT-PCR Core Reagent (ABI) using a sequence detector under the following conditions: sense-primer: 5′-CGGGAGAGCCATAGTGG-3′ (130-S17; Greiner), antisense-primer: 5′-AGTACCACAAG-GCCTTTCG-3′ (290-R19; Greiner), probe: 5′(FAM)-CTGCG-GAACCGGTGAGTACAC (TAMRA)-3′ (148-S21FT; TaKaRa) (Takeuchi et al., 1999), RT-PCR reaction conditions: 50 °C, 2 min→60 °C, 30 min→95 °C, 5 min→45 cycles×(95 °C, 20 s→62 °C, 1 min). The number of copies in the samples was determined using a standard curve calibrated with 10^4 to 10^8 copies of synthesized HCV RNA standards encoding from 5′ terminus to E2 region, and recorded as amount of HCV RNA.

Direct sequencing analysis of HCV replicon RNA

Nucleotide sequences of HCV replicon RNA were analyzed by direct sequencing method. The NS region of total RNA extracted from IFNα-resistant replicon clones was divided into four fragments and amplified using an RT-PCR kit (ReverTra Dash®; TOYOBO). Four primers (HCV-NS-1RV: 5′-ATAGCACT-CGCACAGAACCGA-3′; Greiner, HCV-NS-2RV: 5′-GGAAC-CGTTTTTCACATGTCC-3′; Greiner, HCV-NS-3RV: 5′-ATGTGGTTAACGGCCTTGCT-3′; Greiner, HCV-NS-4RV: 5′-TCATCGGTTGGGGAGTAGATAGA-3′; Greiner) were used for reverse transcription (RT). For polymerase chain reaction (PCR), another four primers (HCV-NS-1FW: 5′-ATGGCGCC-TATTACGGCCTA-3′; Greiner, HCV-NS-2FW: 5′-TGTTC-GATTCCTCGGTTCTGT-3′; Greiner, HCV-NS-3FW: 5′-CCCCTTCTTCTCATGTCAACG-3′; Greiner, HCV-NS-4 FW: 5′-GGAACCTATCCAGCAAGCCC-3′; Greiner) were used in addition to the primers for RT.

RT and PCR reactions were conducted in accordance with the instruction manual provided with the kit. RT reaction was conducted at 42 °C, 20 min, and the reaction mixtures were then heated to 99 °C, 5 min. The PCR reaction was performed for 30 cycles under the following conditions: 98 °C, 10 s; 60 °C, 2 s; then 74 °C, 90 s.

Sequencing was performed using a BigDye Terminator Cycle Sequencing Ready Reaction Kit (ABI). One μL of amplified RT-PCR product for each clone was purified using QIAquick Gel Extraction kit (Qiagen) and the sequence primers were used to prepare each of the reaction solutions in accordance with the manufacturer's procedure. Twenty μL of each solution was allowed to react for 25 cycles under the conditions: 96 °C, 10 s; 50 °C, 5 s; 60 °C, 4 min; then 72 °C, 7 min. The solutions were then purified by Dye EX 2.0 (Qiagen) in accordance with the instruction manual. After that, the samples were applied for sequencing analysis using an ABI PRISM 3100 genetic analyzer (ABI).

The NS region (5952 bp, 1984 amino acids) in sequenced samples underwent gene analysis using Vector NTI analysis software (Invitrogen). In a comparison of deduced amino acid sequences based on nucleotide sequences among the four IFNα-resistant replicon clones and original replicons, the NS regions were compared to that of the original replicon clone to identify mutations. The amino acid sequence of the original replicon cells was included among the materials provided with the Huh-9-13 cell line product from ReBLikon GmbH.

Reporter gene analysis

We attempted to clarify IFNα transactivation in IFNα-resistant replicons. Firefly luciferase fused gene with three repeats of an ISG15-type IFN-stimulated responsive element (ISRE) was used as a reporter construct (pISRE/Luc). HCV replicon cells or Huh-7 cells (3×10^5 cells/well) were seeded on a 60-mm plate in the absence of IFNα. Eight hours after cell seeding, the reporter construct (3 μg) was transfected using FuGENE6 (Roche) as a transfection reagent, following the instruction manual. The transfected cells were cultured further 12 to 14 h, and then the cells (1×10^4 cells) were inoculated on a 96-well plate and cultured for 24 h with or without 1000 IU/mL of IFNα. The luciferase activity was measured by adding Steady Glo® to the cells using TopCount (Packard).

Western blot analysis

The cell lysates were prepared in Laemmli buffer (BIO-RAD) and subjected to SDS-2/15% gradient PAGE and transferred onto nitrocellulose membranes. To detect expression of HCV NS proteins, antibodies against NS3, NS4B, NS5A, and NS5B were used. Anti-β-actin antibody (Sigma) was also used for detection of β-actin as an internal control.

To investigate the phosphorylation of Stat-1 at Tyr701 in HCV replicon cells and its parental Huh-7 cells, the cells were cultured in the medium containing 500 IU/mL of IFNα for 30 min. After cell lysates were prepared as previously described, western blot analysis was performed using an anti-phospho-Stat-1 (Tyr701) antibody (Cell Signaling Technology) or an anti-Stat-1 antibody (BD Transduction Laboratories). Immunocomplexes were detected by visualization using enhanced chemiluminescence (Amersham Biosciences).

Transfection of total RNA derived from replicon cells to naive Huh-7

Total RNA (5 μg) extracted from HCV replicon cells was transfected to Huh-7 cells using DMRIE-C transfection reagents, in accordance with the instruction manuals provided with the reagents. The transfected cells were cultured in the absence of IFNα and selected with 1000 μg/mL of G418 for 4 weeks. Drug-resistant cells were collected and reactivity to IFNα was measured as described in previous section.

Elimination of HCV replicon RNA from replicon cells (Isolation of 'cured' replicon)

To remove HCV replicon RNA from replicon cells, HCV replicon cells were treated ('cured') with HCV RNA-dependent RNA polymerase NS5B inhibitor, JTP-71892, JTK-109-derivatives synthesized in our laboratory (Hirashima et al., 2006; Ishida et al., 2006). The replicon cells (5×10^4 cells) were inoculated on a 60-mm plate and further cultured in the presence of the compound (1 μM) for about 4 weeks. The cell culture was performed in the absence of G418, to prevent survival of the compound-resistant clones. Medium was exchanged with fresh medium containing the compound twice per week. The finding that 1 μM of JTP-71892 does not exhibit any toxicity or growth inhibition in long-term culture had been previously confirmed.

Acknowledgments

We thank M. Tomonaga, Y. Hori and K. Asahina for their technical assistance in this work. We also greatly acknowledge Dr. R. Bartenschlager for providing us the HCV subgenomic replicon (Huh-9-13) and naive Huh-7 cell lines for parental cell line of Huh-9-13.

References

Alter, M.J., 1997. Epidemiology of hepatitis C. Hepatology 26, 62S–65S.

Appel, N., Pietschmann, T., Bartenschlager, R., 2005. Mutational analysis of hepatitis C virus nonstructural protein 5A: potential role of differential phosphorylation in RNA replication and identification of a genetically flexible domain. J. Virol. 79, 3187–3194.

Asabe, S., Tanji, Y., Satoh, S., Kaneko, T., Kimura, K., Shimotohno, K., 1997. The N-terminal region of hepatitis C virus-encoded NS5A is important for NS4A dependent phosphorylation. J. Virol. 71, 790–796.

Bartenschlager, R., Lohmann, V., 2000. Replication of hepatitis C virus. J. Gen. Virol. 81, 1631–1648.

Bartenschlager, R., Lohmann, V., 2001. Novel cell culture systems for the hepatitis C virus. Antivir. Res. 52, 1–17.

Choo, Q.L., Richman, K.H., Han, J.H., Berger, K., Lee, C., Dong, C., Gallegos, C., Coit, D., Medina, S.R., Barr, P.J., Weiner, A.J., Bradely, D.W., Kuo, G., Houghton, M., 1991. Genetic organization and diversity of the hepatitis C virus. Proc. Natl. Acad. Sci. U. S. A. 88, 2451–2455.

Enomoto, N., Sakuma, I., Asahina, Y., Kurosaki, M., Murakami, T., Yamamoto, C., Ogura, Y., Izumi, N., Marumo, F., Sato, C., 1996. Mutations in the nonstructural protein 5A gene and response to interferon I patients with chronic hepatitis C virus 1b infection. N. Engl. J. Med. 334, 77–81.

Evans, M.J., Rice, C.M., Goff, S.P., 2004. Phosphorylation of hepatitis C virus nonstructural protein 5A modulates its protein interactions and viral RNA replication. Proc. Natl. Acad. Sci. U. S. A. 101, 13038–13043.

Frese, M., Schwärzle, V., Barth, K., Krieger, N., Lohmann, V., Mihm, S., Haller, O., Bartenschlager, R., 2002. Interferon-γ inhibits replication of subgenomic and genomic hepatitis C virus RNAs. Hepatology 35, 694–703.

Gale, M.J., Korth, M.J., Tang, N.M., Tan, S.L., Hopkins, D.A., Dever, T.E., Polyak, S.J., Gretch, D.R., Katze, M.G., 1997. Evidence that hepatitis C virus resistance to interferon is mediated through repression of the PKR protein kinase by nonstructural 5A protein. Virology 230, 217–227.

Gong, G.Z., Cao, J., Jiang, Y.F., Zhou, Y., Liu, B., 2007. Hepatitis C virus nonstructural 5A abrogates signal transducer and activator of transcription-1 nuclear translocation induced by IFN-alpha through dephosphorylation. World Gastroenterol. 13, 4080–4084.

Guo, J.T., Bichko, V.V., Seeger, C., 2001. Effect of alpha interferon on the hepatitis C virus replicon. J. Virol. 75, 8516–8523.

Guo, J.T., Sohn, J.A., Zhu, Q., Seeger, C., 2004. Mechanism of the interferon alpha response against hepatitis C virus replicons. Virology 325, 71–81.

Hijikata, M., Kato, N., Ootsuyama, Y., Nakagawa, M., Shimotohno, K., 1991. Gene mapping of the putative structural region of the hepatitis C virus genome by *in vitro* processing analysis. Proc. Natl. Acad. Sci. U. S. A. 88, 5547–5551.

Hijikata, M., Mizushima, H., Tanji, Y., Komoda, Y., Hirowatari, Y., Akagi, N., Kato, N., Kimura, K., Shimotohno, K., 1993a. Proteolytic processing and membrane association of putative nonstructural proteins of hepatitis C virus. Proc. Natl. Acad. Sci. U. S. A. 90, 10773–10777.

Hijikata, M., Mizushima, H., Tanji, Y., Komoda, Y., Hirowatari, Y., Akagi, N., Kato, N., Kimura, K., Shimotohno, K., 1993b. Two distinct proteinase activities required for the processing of a putative nonstructural precursor protein of hepatitis C virus. J. Virol. 67, 4665–4675.

Hirashima, S., Suzuki, T., Ishida, T., Noji, S., Yata, S., Ando, I., Komatsu, M., Ikeda, S., Hashimoto, H., 2006. Benzimidazole derivatives bearing substituted biphenyls as hepatitis C virus NS5B RNA-dependent RNA polymerase inhibitors: structure-activity relationship studies and identification of a potent and highly selective inhibitor JTK-109. J. Med. Chem. 49, 4721–4736.

Houghton, M., 1996. Hepatitis C viruses. p1035–1058, In: Fields, B.N., Knipe, D.M., Howley, P.M. (Eds.), Fields Virology. 3rd ed. Lippincott-Raven Co., Philadelphia.

Huang, Y., Chen, X.C., Konduri, M., Fomina, N., Lu, J., Jin, L., Kolykhalov, A., Tan, S.L., 2006. Mechanistic link between the anti-HCV effect of interferon gamma and control of viral replication by a Ras-MAPK signaling cascade. Hepatology 43, 81–90.

Ide, Y., Tanimoto, A., Sasaguri, Y., Padmanabhan, R., 1997. Hepatitis C virus NS5A protein is phosphorylated in vitro by a stably bound protein kinase from HeLa cells and by cAMP-dependent protein kinase A-a catalytic subunit. Gene 201, 151–158.

Ishida, T., Suzuki, T., Hirashima, S., Mizutani, K., Yoshida, A., Ando, I., Ikeda, S., Adachi, T., Hashimoto, H., 2006. Benzimidazole inhibitors of hepatitis C

virus NS5B polymerase: identification of 2-[(4-diarylmethoxy) phenyl]-benzimidazole. Bioorg. Med. Chem. Lett. 16, 1859–1863.
Kaneko, T., Tanji, Y., Satoh, S., Hijikata, M., Asabe, S., Kimura, K., Shimotohno, K., 1994. Production of two phosphoproteins from the NS5A region of the hepatitis C virus genome. Biochem. Biophys. Res. Commun. 205, 320–326.
Kato, N., Hijikata, M., Ootsuyama, M., Nakagawa, S., Ohkoshi, S., Suginmura, T., Shimotohno, K., 1990. Molecular cloning of the human hepatitis C virus genome from Japanese patients with non-A, non-B hepatitis. Proc. Natl. Acad. Sci. U. S. A. 87, 9524–9528.
Kawai, T., Takahashi, K., Sato, S., Coban, C., Kumar, H., Kato, H., Ishii, K.J., Takeuchi, O., Akira, S., 2005. IPS-1, an adaptor triggering RIG-I- and Mda5-mediated type I interferon induction. Nat. Immunol. 6, 1074–1076.
Kim, J., Lee, D., Choe, J., 1999. Hepatitis C virus NS5A protein is phosphorylated by casein kinase II. Biochem. Biophys. Res. Commun. 257, 777–781.
Lan, K.H., Lan, K.L., Lee, W.P., Sheu, M.L., Chen, M.Y., Lee, Y.L., Yen, S.H., Chang, F.Y., Lee, S.D., 2007. HCV NS5A inhibits interferon-alpha signaling through suppression of STAT1 phosphorylation in hepatocyte-derived cell lines. J. Hepatol. 46, 759–767.
Lindsay, K.L., 1997. Therapy of hepatitis C: overview. Hepatology 26, 71S–77S.
Lohmann, V., Körner, F., Koch, J., Herian, U., Theilman, L., Bartenschlager, R., 1999. Replication of subgenomic Hepatitis C virus RNAs in a hepatoma cell line. Science 285, 110–113.
McHutchison, J.G., Gordon, S.C., Schiff, E.R., Shiffman, M.L., Lee, W.M., Rustgi, V.K., Goodman, Z.D., Ling, M.H., Cort, S., Albrecht, J.K., 1998. Interferon alfa-2b alone or in combination with ribavirin as initial treatment for chronic hepatitis C. Hepatitis Interventional Therapy Group. N. Engl. J. Med. 339, 1485–1492.
Meylan, E., Curran, J., Hofmann, K., Moradpour, D., Binder, M., Bartenschlager, R., Tschopp, J., 2005. Cardif is an adaptor protein in the RIG-I antiviral pathway and is targeted by hepatitis C virus. Nature 437, 1167–1172.
Naka, K., Takemoto, K., Abe, K., Dansako, H., Ikeda, M., Shimotohno, K., Kato, N., 2005. Interferon resistance of hepatitis C virus replicon-harboring cells is caused by functional disruption of type I interferon receptors. J. Gen. Virol. 86, 2787–2792.
Namba, K., Naka, K., Dansako, H., Nozaki, A., Ikeda, M., Shiratori, Y., Shimotohno, K., Kato, N., 2004. Establishment of hepatitis C virus replicon cell lines possessing interferon-resistant phenotype. Biochem. Biophys. Res. Commun. 323, 299–309.
Neddermann, P., Quintavalle, M., Di Pietro, C., Clementi, A., Cerretani, M., Altamura, S., Bartholomew, L., De Francesco, R., 2004. Reduction of hepatitis C virus NS5A hyperphosphorylation by selective inhibition of cellular kinases activates viral RNA replication in cell culture. J. Virol. 78, 13306–13314.
Noguchi, T., Satoh, S., Noshi, T., Hatada, E., Fukuda, R., Kawai, A., Ikeda, S., Hijikata, M., Shimotohno, K., 2001. Effects of mutation in hepatitis C virus nonstructural protein 5A on interferon resistance mediated by inhibition of PKR kinase activity in mammalian cells. Microbiol. Immunol. 45, 829–840.
Nousbaum, J., Polyak, S.J., Ray, S.C., Sullivan, D.G., Larson, A.M., Caritherns, R.L., Gretch, D.R., 2000. Prospective characterization of full-length hepatitis C virus NS5A quasispecies during induction and combination antiviral therapy. J. Virol. 74, 9028–9038.
Okamoto, H., Okada, S., Sugiyama, Y., Kurai, K., Iizuka, H., Machida, A., Miyakawa, Y., Tsuda, F., Mayumi, M., 1991. Nucleotide sequence of the genomic of hepatitis C virus isolated from a human carrier: comparison with reported isolates for conserved and divergent regions. J. Gen. Virol. 72, 2697–2704.
Okamoto, H., Kurai, K., Okada, S., Yamamoto, K., Iizuka, H., Tanaka, T., Fukuda, S., Tsuda, F., Mishiro, S., 1992. Full-length sequence of a hepatitis C virus genome having poor homology to reported isolates: comparative study of four distinct genotypes. Virology 188, 331–341.
Puig-Basagoiti, F., Forns, X., Furcic, I., Ampurdanes, S., Gimenez-Barcons, M., Franco, S., Sanchez-Tapias, J.M., Saiz, J.C., 2005. Dynamics of hepatitis C virus NS5A quasispecies during interferon and ribavirin therapy in responder and non-responder patients with genotype 1b chronic hepatitis C. J. Gen. Virol. 86, 1067–1075.
Reed, K.E., Xu, J., Rice, C.M., 1997. Phosphorylation of the hepatitis C virus NS5A protein in vitro and in vivo: properties of the NS5A-associated kinase. J. Virol. 71, 7187–7197.
Reed, K.E., Gorbalenya, A.E., Rice, C.M., 1998. The NS5A/NS5 proteins of viruses from three genera of the family *Flaviviridae* are phosphorylated by associated serine/threonine kinases. J. Virol. 72, 6199–6206.
Sarcar, B., Ghosh, A.K., Steele, R., Ray, R., Ray, R.B., 2004. Hepatitis C virus NS5A mediated STAT3 activation requires co-operation of Jak1 kinase. Virology 322, 51–60.
Seth, R.B., Sun, L., Ea, C.K., Chen, Z.J., 2005. Identification and characterization of MAVS, a mitochondrial antiviral signaling protein that activates NF-kappaB and IRF 3. Cell 122, 669–682.
Sumpter Jr., R., Wang, C., Foy, E., Loo, Y.M., Gale Jr., M., 2004. Viral evolution and interferon resistance of hepatitis C virus RNA replication in a cell culture model. J. Virol. 78, 11591–11604.
Taguchi, T., Nagano-Fujii, M., Akutsu, M., Kadoya, H., Ohgimoto, S., Ishido, S., Hotta, H., 2004. Hepatitis C virus NS5A protein interacts with 2′, 5′-oligoadenylate synthetase and inhibits antiviral activity of IFN in an IFN sensitivity-determining region-independent manner. J. Gen. Virol. 85, 959–969.
Takamizawa, A., Mori, C., Fuke, I., Manabe, S., Murakami, S., Fujita, J., Onishi, E., Andoh, T., Yoshida, I., Okayama, H., 1991. Structure and organization of the hepatitis C virus genome isolated from human carriers. J. Virol. 65, 1105–1113.
Takeuchi, T., Katsume, A., Tanaka, T., Abe, A., Inoue, K., Tsukiyama-Kohara, K., Kawaguchi, R., Tanaka, S., Kohara, M., 1999. Real-time detection system for quantification of hepatitis C virus genome. Gastroenterology 116, 636–642.
Tanji, Y., Kaneko, T., Satoh, S., Shimotohno, K., 1995. Phosphorylation of hepatitis C virus-encoded nonstructural protein NS5A. J. Virol. 69, 3980–3986.
Tong, C.Y., Gilmore, I.T., Hart, C.A., 1995. HCV-associated liver cancer. Lancet 345, 1058–1059.
Xu, L.G., Wang, Y.Y., Han, K.J., Li, L.Y., Zhai, Z., Shu, H.B., 2005. VISA is an adapter protein required for virus-triggered IFN-beta signaling. Mol. Cell 19, 727–740.
Yoneyama, M., Kikuchi, M., Natsukawa, T., Shinobu, N., Imaizumi, T., Miyagishi, M., Taira, K., Akira, S., Fujita, T., 2004. The RNA helicase RIG-I has an essential function in double-stranded RNA-induced innate antiviral responses. Nat. Immunol. 5, 730–737.
Zhu, H.m., Nelson, D.R., Crawford, J.M., Liu, C., 2005. Defective Jak-Stat activation in hepatoma cells is associated with hepatitis C viral IFN-alpha resistance. J. Interferon Cytokine Res. 25, 528–539.

THE JOURNAL OF BIOLOGICAL CHEMISTRY VOL. 283, NO. 49, pp. 34273–34282, December 5, 2008

Human T-cell Leukemia Virus Type 1 HBZ Protein Bypasses the Targeting Function of Ubiquitination*

Received for publication, April 1, 2008, and in revised form, September 5, 2008 Published, JBC Papers in Press, September 19, 2008, DOI 10.1074/jbc.M802527200

Osamu Isono[‡], Takayuki Ohshima[‡§], Yasushi Saeki[¶], Jun Matsumoto[‡], Makoto Hijikata[‡], Keiji Tanaka[¶], and Kunitada Shimotohno[‡‖1]**

*From the [‡]Laboratory of Human Tumor Viruses, Department of Viral Oncology, Institute for Virus Research, Kyoto University, Sakyo-ku, Kyoto 606-8507, the [§]Faculty of Pharmaceutical Science at Kagawa Campus, Tokushima Bunri University, Sanuki, Kagawa 769-2193, the [¶]Laboratory of Frontier Science, Core Technology and Research Center, Tokyo Metropolitan Institute of Medical Science, Bunkyo-ku, Tokyo 113-8613, the [‖]Center for Integrated Medical Research, School of Medicine, Keio University, Shinjuku-ku, Tokyo 160-8582, and the **Research Institute, Chiba Institute of Technology, Narashino, Chiba 275-0016, Japan*

Human T-cell leukemia virus type 1 (HTLV-1) encodes an antisense viral gene product termed HTLV-1 basic leucine-zipper factor (HBZ). HBZ forms heterodimers with c-Jun, a member of the AP-1 family, and promotes its proteasomal degradation. Although most proteasomal substrates are targeted for degradation via conjugation of polyubiquitin chains, we show that ubiquitination is not required for HBZ-mediated proteasomal degradation of c-Jun. We demonstrate that HBZ directly interacts with both the 26 S proteasome and c-Jun and facilitates the delivery of c-Jun to the proteasome without ubiquitination. HBZ acts as a tethering factor between the 26 S proteasome and its substrate, thereby bypassing the targeting function of ubiquitination. These findings disclose a novel viral strategy to utilize the cellular proteolytic system for viral propagation.

Protein degradation plays a variety of roles in fundamental cellular processes, including the cell cycle, apoptosis, immune response, and disposal of misfolded or oxidized proteins (1–3). The ubiquitin-proteasome system has evolved as a key machinery in the selective degradation of intracellular short-lived regulatory or abnormal proteins. Most proteasomal substrates are tagged with polyubiquitin, which serves as a recognition signal for the 26 S proteasome. The cellular machinery that adds ubiquitin to substrates consists of three main enzyme classes. The E1 ubiquitin-activating enzyme transfers activated ubiquitin to the E2 ubiquitin-conjugating enzyme, which, in combination with E3 ubiquitin ligase, transfers ubiquitin to the substrate. The E3 ubiquitin ligase associates with the substrate and confers substrate specificity (3).

The proteasome is a major nonlysosomal proteolytic apparatus. The catalytic core of this multisubunit proteolytic complex is the 20 S proteasome. The addition of a 19 S regulatory complex to either or both ends of the 20 S proteasome forms the 26 S proteasome. The 19 S regulatory complex recognizes polyubiquitin chains on substrates and catalyzes deubiquitination, denaturation, and translocation of the unfolded substrate into the 20 S catalytic core for degradation (4). Thus, the substrates for the actual proteolysis are unfolded and nonubiquitinated. Therefore, if a protein can be delivered to the proteasome in a denatured or partially unfolded state, ubiquitination should not be required for its degradation (5, 6). Recently, there have been emerging reports of proteasome-dependent, ubiquitin-independent degradation of eukaryotic proteins (7), including ornithine decarboxylase (ODC)[2] (8), p53 (9), $p21^{waf1/cip1}$ (10, 11), and retinoblastoma (Rb) protein (12, 13), suggesting the significance of this alternative pathway for various cellular events. However, the mechanism by which proteasomes recognize nonubiquitinated substrates is not well understood.

A variety of viruses are known to utilize the host ubiquitin-proteasome system to dysregulate cellular functions for their benefit. Notably, human papillomavirus type-16 E6 protein acts as a part of the E3 ubiquitin ligase complex to promote ubiquitination and subsequent degradation of the tumor suppressor, p53 (14). There are an increasing number of viral proteins that utilize cellular ubiquitination machinery (15–17), suggesting that the cellular proteolytic system is an important tool for viral propagation.

Human T-cell leukemia virus type-1 (HTLV-1) causes adult T-cell leukemia in 2–5% of carriers after a long latent period (18). HTLV-1-induced disruption of cellular transcription is associated with the development of adult T-cell leukemia. Tax, one of the HTLV-1-encoded proteins, is postulated to play a pivotal role in the development of adult T-cell leukemia (19). Although Tax promotes proliferation and inhibits apoptosis of infected cells, it is a

* This work was supported by grants-in-aid for cancer research and for the second-term comprehensive 10-year strategy for cancer control from the Ministry of Health, Labour and Welfare as well as by grants-in-aid for Scientific Research on Priority Areas "Integrative Research Toward the Conquest of Cancer" from the Ministry of Education, Culture, Sports, Science and Technology of Japan. In addition, this work was supported by research funds from the Takeda Science Foundation, the Suzuken Memorial Foundation, and the Japanese Leukemia Research Foundation. The costs of publication of this article were defrayed in part by the payment of page charges. This article must therefore be hereby marked "*advertisement*" in accordance with 18 U.S.C. Section 1734 solely to indicate this fact.

[1] To whom correspondence should be addressed. Tel.: 81-3-5363-3591; Fax: 81-3-5363-3592; E-mail: shimkuni@z8.keio.jp.

[2] The abbreviations used are: ODC, ornithine decarboxylase; Rb, retinoblastoma; GST, glutathione *S*-transferase; Ub, ubiquitin; Ni-NTA, nickel-nitrilotriacetic acid; CMV, cytomegalovirus; HA, hemagglutinin; CREB, cAMP-response element-binding protein; GADD34, growth arrest and DNA damage-inducible transcript 34; MCM5, minichromosome maintenance protein 5; AP-1, activating protein-1; HTLV-1, human T-cell leukemia virus type 1; HBZ, HTLV-1 bZIP factor.

major target of cytotoxic T lymphocytes (20), thus the overexpression of viral protein is disadvantageous for the survival of infected cells. There are significant involvements of other viral factors that control viral expression (21, 22). Recently, a novel viral protein, HTLV-1 basic leucine-zipper factor (HBZ), which is encoded in the complementary strand of the HTLV-1 genome, was identified (23). HBZ is a nuclear protein that contains a transactivation domain and a basic leucine-zipper (bZIP) domain in its N and C termini, respectively. HBZ interacts with cellular bZIP proteins, particularly the AP-1 family of transcription factors, and regulates their transcriptional activities, allowing the virus to control viral gene transcription from the HTLV-1 promoter (23–25). We previously reported that HBZ interacts with c-Jun, an AP-1 family member, and suppresses its transcriptional activity by two distinct mechanisms. HBZ not only impairs the DNA-binding activity of c-Jun but also promotes its proteasomal degradation (26).

In this study, we show that ubiquitination is not required for HBZ-mediated proteasomal degradation of c-Jun. We demonstrate that HBZ directly interacts with both the 26 S proteasome and c-Jun and facilitates the delivery of c-Jun to the proteasome without ubiquitination. HBZ acts as a tethering factor between the 26 S proteasome and its substrate, thereby bypassing the targeting function of ubiquitination.

EXPERIMENTAL PROCEDURES

Cell Culture, Transfection, and Reagents—HEK-293T cells were cultured in Dulbecco's modified Eagle's medium (Nissui) supplemented with 10% fetal bovine serum (Invitrogen), 4 mM L-glutamine, and 0.1 mg/ml kanamycin sulfate at 37 °C in a 5% CO_2 atmosphere. Mouse ts20 cells (kindly provided by Dr. Harvey Ozer) were cultured similarly, but maintained at 35 °C (the permissive temperature). C8166 cells were maintained in RPMI 1640 medium (Nissui) supplemented with 10% fetal bovine serum and 4 mM L-glutamine. Transfections were performed using FuGENE6 (Roche Applied Sciences) for HEK-293T cells, or Lipofectamine 2000 (Invitrogen) for ts20 cells following the manufacturer's protocol. However, in the experiment in Fig. 1*B*, HEK-293T cells were transfected with Lipofectamine 2000. Cells were treated with the proteasome inhibitor MG132 (20 μM, Peptide Institute) for 12 h prior to collection.

Plasmids—pcDNA3-FLAG-HBZ, pcDNA3-HA-c-Jun, and pcDNA3-c-Jun-Myc-His have been described previously (26). Deletions and point mutants of HBZ and c-Jun were generated by PCR amplification of pcDNA3-FLAG-HBZ and pcDNA3-HA-c-Jun, respectively. These PCR fragments were then subcloned into expression vectors such as pcDNA3-FLAG, pcDNA3-HA, pcDNA3-His (Invitrogen), pGEX-6P-1 (Amersham Biosciences), or pGBT9 (Clontech). In addition, pcDNA3-FLAG-HBZ-SI was generated by PCR using pcDNA3-FLAG-HBZ as a template. The cDNAs were amplified by reverse transcription-PCR using total RNA from MT-2 cells (for c-Jun, JunB, JunD, c-Fos, ATF1, ATF2, ATF4, CREB, p53, and GADD34), 293T cells (for ubiquitin, Rpn5, MCM5, MCM7, and DET1), and Saos-2 cells (for COP1). They were subcloned into pcDNA3-FLAG, pcDNA3-Myc, pcDNA3-HA, pcDNA3-His, or pCAG vectors. Site-directed mutagenesis was used to generate the dominant-negative ubiquitin mutant (Ub-K48R), which contains an Arg substitution at Lys-48. To generate pcDNA3-FLAG-c-JunLZ/p53, the fragment encoding the c-Jun leucine-zipper region (273–310 amino acids) was PCR-amplified from pcDNA3-HA-c-Jun, digested with BamHI, and subcloned in-frame into BamHI-linearized pcDNA3-FLAG-p53.

Immunoblot Analysis—Proteins were fractionated by SDS-PAGE, transferred to a polyvinylidene difluoride membrane, and hybridized with the appropriate primary and horseradish peroxidase-conjugated secondary antibodies for subsequent detection by enhanced chemiluminescence (ECL, PerkinElmer Life Sciences). The antibodies used in this study were specific for FLAG (M2, Sigma), Myc (9E10, Santa Cruz Biotechnology), HA (3F10, Roche Applied Science), α-tubulin (Ab-1, Calbiochem), c-Jun (H-79, Santa Cruz Biotechnology), c-Fos (sc-52, Santa Cruz Biotechnology), α3 (MCP257, Affiniti Research Products), α7 (MCP72, Affiniti), Rpt6 (p45–110, Affiniti), and Rpn10 (S5a-18, Affiniti). Horseradish peroxidase-conjugated goat antibodies to mouse, rabbit, or rat IgG were obtained from Amersham Biosciences.

Immunoprecipitations—Cells were lysed in 1 ml of lysis buffer, which contained 50 mM Tris-HCl (pH 8.0), 100 mM NaCl, 1 mM EDTA, 0.5% Nonidet P-40, 1 mM dithiothreitol, 1 mM phenylmethylsulfonyl fluoride, 50 mM sodium fluoride, 2 mM sodium orthovanadate, and a protease inhibitor mixture (Complete EDTA-free, Roche Applied Science) at 4 °C for 30 min. After centrifugation, the supernatant was incubated with 10 μl of agarose-immobilized anti-FLAG (M2, Sigma) or anti-HA (Sigma) antibodies at 4 °C for 3 h. Resins were washed four times with 700 μl of lysis buffer. Bound proteins were eluted by boiling for 10 min in 1× sample buffer (62.5 mM Tris-HCl (pH 6.8), 2% SDS, 10% glycerol, and 5% 2-mercaptoethanol) and then subjected to SDS-PAGE, followed by immunoblot analysis.

Pulse-Chase Analysis—HEK-293T cells were seeded on 6-well plates (3×10^5 cells/well) and transfected with the appropriate expression plasmids. After 24 h, cells were labeled metabolically for 1 h with 100 μCi of [^{35}S]methionine/cysteine (ICN) in methionine/cysteine-free Dulbecco's modified Eagle's medium (ICN) supplemented with 10% dialyzed fetal bovine serum and 4 mM L-glutamine. After washing with phosphate-buffered saline, cells were chased for the indicated intervals in complete medium. Harvested cells were then solubilized with lysis buffer that also contained 0.1% SDS and 0.5% sodium deoxycholate. The soluble fractions were incubated for 1 h with 2 μg of anti-c-Myc antibody and adsorbed to protein G-Sepharose (Amersham Biosciences). Immunoprecipitates were resolved by SDS-PAGE and detected by autoradiography. Band intensities were measured with scanning densitometry (Fluor-S Multilmager, Bio-Rad).

Glutathione S-Transferase Pulldown Assay—GST and GST fusion proteins were expressed in *Escherichia coli* strain BL21 and affinity-purified using glutathione-Sepharose beads (Amersham Biosciences). For *in vitro* translation, [^{35}S]methionine (Amersham Biosciences)-labeled proteins were produced using the TnT quick-coupled transcription/translation system (Promega). *In vitro* translated proteins were incubated at 4 °C for 3 h with GST or GST fusion protein in 700 μl of GST-binding buffer containing 20 mM Tris-HCl (pH 8.0), 0.5%

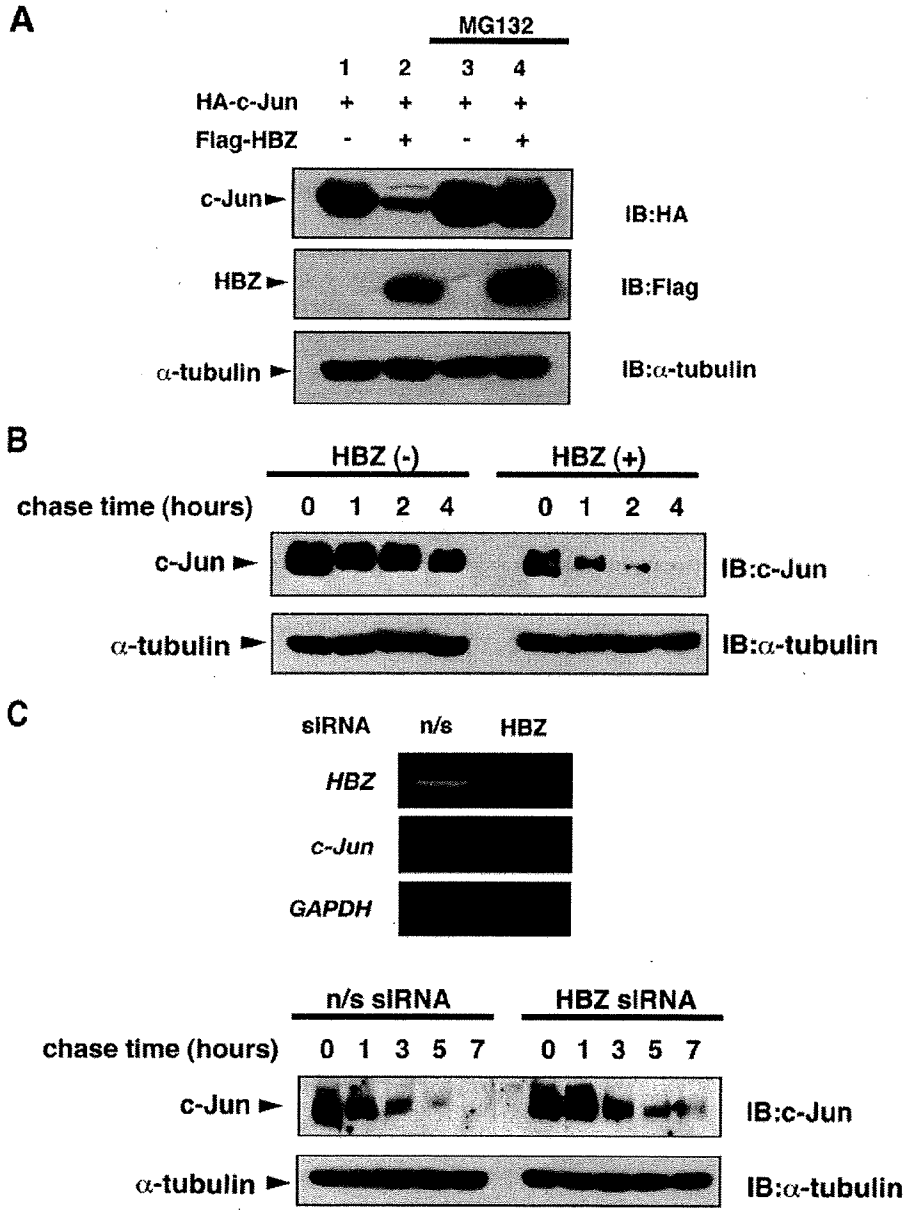

FIGURE 1. **HBZ promotes proteasomal degradation of c-Jun.** *A*, HEK-293T cells were transfected with 0.5 μg of pcDNA3-HA-c-Jun and 3 μg of either pcDNA3 or pcDNA3-FLAG-HBZ. After 12 h, the cells were treated with or without MG132 for 12 h. Cell lysates were immunoblotted with the antibodies indicated. *B*, HEK-293T cells were transfected with 5 μg of pCAG-FLAG-HBZ or control vector. After 36 h, the cells were treated with cycloheximide (50 μg/ml) and collected at the indicated times. Cell lysates were analyzed by immunoblot analysis. *C, upper panel*: C8166 cells were transfected using lentiviruses transcribing short hairpin RNAs against HBZ or a nonspecific (*n/s*) sequence. The relative mRNA expression of HBZ, c-Jun or glyceraldehyde-3-phosphate dehydrogenase (*GAPDH*) was evaluated by semiquantitative reverse transcription-PCR 7 days after transfection. Efficiencies of lentivirus vector transfection, which were determined by green fluorescent protein expression, were >95%. *Lower panel*: C8166 cells were transfected as indicated in the *upper panel*. After 7 days, the cells were treated with cycloheximide (50 μg/ml) and collected at the indicated times. Cell lysates were analyzed by immunoblot analysis.

Nonidet P-40, 150 mM NaCl, 1 mM EDTA, 1 mM dithiothreitol, 10% glycerol, 1 mM phenylmethylsulfonyl fluoride, and a protease inhibitor mixture. Beads were washed three times with GST-binding buffer, and then bound proteins were resolved by SDS-PAGE and detected by autoradiography.

In Vivo Ubiquitination Assay—HEK-293T cells were transfected with pcDNA3-His-c-Jun or pcDNA3-His-c-Fos, pcDNA3-HA-HBZ, and pcDNA3-FLAG-ubiquitin (Ub) in different combinations. After treatment with MG132 (20 μM) for 12 h, cells were lysed in buffer A (8 M urea, 10 mM imidazole, 0.5% Triton X-100, 100 mM Hepes (pH 7.5)) and incubated with 20 μl of Ni-NTA beads (Qiagen) for 2 h at room temperature. The beads were washed with buffer B (8 M urea, 50 mM imidazole, 0.5% Triton X-100, 100 mM Hepes (pH 7.5), 0.5 M NaCl). The bound proteins were eluted with buffer C (8 M urea, 500 mM imidazole, 100 mM Hepes (pH 7.5)) and then subjected to SDS-PAGE, followed by immunoblot analysis.

Degradation Analysis in Temperature-sensitive ts20 Cells—ts20 cells in 10-cm plates were transfected with the appropriate expression plasmids and incubated for 12 h at 35 °C (permissive temperature). Cells were split into two dishes and incubated for an additional 12 h at 35 °C. Then, appropriate plates were moved to the restrictive temperature (39 °C). Cells were harvested after 24 h and subjected to SDS-PAGE, followed by immunoblot analysis.

Yeast Two-hybrid Screen—A human spleen cDNA library fused to the GAL4 activation domain of pACT2 (Clontech) was screened against the bait protein, the GAL4 DNA-binding domain fused to the HBZ N-terminal 120 amino acids (pGBT9-HBZ-N). pGBT9-HBZ-N and the cDNA library were co-introduced into the yeast cell line Y190 using the lithium acetate transformation method (27). The transformants were plated onto selective medium lacking histidine, tryptophan, and leucine, and containing 150 mM 3-aminotriazole to isolate clones with histidine prototrophy. Selected clones were assayed for another marker, β-galactosidase activity, as described in the Clontech protocol. Plasmid DNA was extracted from positive clones and analyzed by partial DNA sequencing.

Glycerol Density Gradient Analysis—HEK-293T cells transiently expressing HA-tagged HBZ were lysed in 1 ml of lysis buffer containing 25 mM Tris-HCl (pH 7.5), 1 mM dithiothreitol, 2 mM ATP, and 0.2% Nonidet P-40. After centrifugation, the

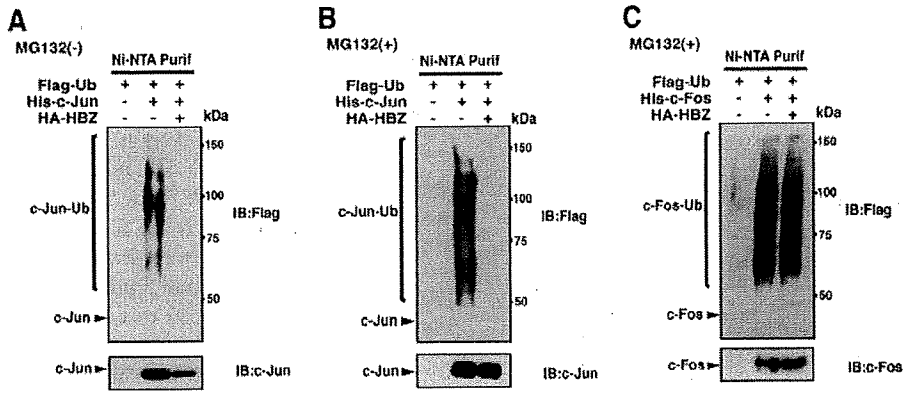

FIGURE 2. **HBZ does not promote the ubiquitination of c-Jun.** *A*, HEK-293T cells were transfected with 2 μg of pcDNA3-His-c-Jun, pcDNA3-FLAG-Ub, and pcDNA3-HA-HBZ as indicated. Following purification with Ni-NTA beads, bound proteins were detected by immunoblot analysis. *B*, HEK-293T cells were transfected as indicated in *A*. After 12 h, the cells were treated with MG132 for 12 h. Following Ni-NTA purification, bound proteins were detected by immunoblot analysis. *C*, HEK-293T cells were transfected with 2 μg of pcDNA3-His-c-Fos, pcDNA3-FLAG-Ub, and pcDNA3-HA-HBZ as indicated. After 12 h, the cells were treated with MG132 for 12 h. Following Ni-NTA purification, bound proteins were detected by immunoblot analysis.

supernatant was subjected to 10–40% (v/v) glycerol density gradient centrifugation in a Hitachi RPS40T rotor (22 h, 83,000 × *g*). The gradient was separated into 30 fractions from the bottom.

Lentiviral Vector Construction and Transfection—The lentivirus-based transfection system was a generous gift from Dr. H. Miyoshi. To express short hairpin RNAs against HBZ, complementary DNA oligonucleotides were inserted into the lentiviral vector (pCS-RfA-EG) under control of the H1 promoter. The target sequence against HBZ was 5′-GCAGATTGCTGAGTATTTG-3′. We cotransfected 4.5 μg of the above lentiviral vector (pCS-RfA-EG-shHBZ) with 3.5 μg of pMDLg/pRRE and 1.5 μg of pCMV-VSV-G-RSV-Rev into packaging cells (293FT) using Lipofectamine 2000. After a 48-h incubation, the culture medium was harvested and concentrated 100- to 200-fold by ultrafiltration. The titer of concentrated virus was measured on 293T cells based on their green fluorescent protein expression. Cells were transfected at a multiplicity of infection of 30 in the presence of Polybrene (4 μg/ml, Sigma). Cells were collected 7 days later, and green fluorescent protein expression was analyzed by FACSCalibur instrument (BD Biosciences).

RNA Isolation and Reverse Transcription-PCR—After 7 days of lentiviral infection, total RNA was extracted with Sepasol RNA I super reagent (Nacalai Tesque). We evaluated the relative expression of each mRNA by semiquantitative reverse transcription-PCR using a One-step RNA PCR kit (Takara). The following primers were used. HBZ: 5′-GAGAAGAAGGCCGCTGAC-3′ and 5′-TTATTGCAACCACATCGC-3′, c-Jun: 5′-GAACTGCACAGCCAGAAC-3′ and 5′-GGCGATTCTCTCCAGCTT-3′, and glyceraldehyde-3-phosphate dehydrogenase: 5′-ATGGGGAAGGTGAAGGTCGG-3′ and 5′-TGGAGGGATCTCGCTCCTGG-3′.

RESULTS

HBZ Promotes Proteasomal Degradation of c-Jun—We previously showed that HBZ heterodimerized with c-Jun via respective leucine-zipper domains and targeted c-Jun for proteasomal degradation (26). When c-Jun and HBZ were ectopically coexpressed in cells, c-Jun expression was significantly reduced. The reduction in c-Jun protein levels by HBZ was prevented by treating with the proteasome inhibitor, MG132, as confirmed in Fig. 1*A*. In addition, ectopically expressed HBZ reduced the half-life of endogenous c-Jun in HEK-293T cells (Fig. 1*B*). We next evaluated the effect of HBZ on c-Jun stability in HTLV-1-infected cells. We suppressed the HBZ gene in HTLV-1-infected C8166 cells by using lentivirus vector transcribing short hairpin RNAs against HBZ (Fig. 1*C*, *upper panel*). As shown in Fig. 1*C* (*lower panel*), HBZ knockdown prolonged the half-life of endogenous c-Jun in C8166 cells. These results indicate that HBZ regulates c-Jun stability by promoting its proteasomal degradation.

HBZ Does Not Promote the Ubiquitination of c-Jun—Most proteasomal substrates are targeted for degradation by the conjugation of polyubiquitin chains (28). The conjugation reaction is catalyzed by a variety of E3 ubiquitin ligases. Because c-Jun is also degraded by a ubiquitin-proteasome pathway that is mediated by several E3 ubiquitin ligases (29, 30), we speculated that HBZ acts as a component of E3 ubiquitin ligase. Therefore, we examined whether HBZ promotes polyubiquitination of c-Jun. Histidine-tagged c-Jun and epitope-tagged HBZ and ubiquitin were co-expressed in HEK-293T cells in different combinations. After purification with Ni-NTA beads, polyubiquitinated c-Jun species were specifically detected by immunoblotting. Interestingly, not only did we not detect an increase, but we also were unable to detect any ubiquitinated species of c-Jun in the presence of HBZ (Fig. 2*A*). This is not likely due to decreased c-Jun protein levels, because we also failed to detect any ubiquitinated c-Jun species in the presence of HBZ even after the treatment with MG132 (Fig. 2*B*). However, this abrogation of ubiquitination did not seem to be the result of a global inhibition of ubiquitination machinery, because HBZ did not alter the ubiquitination level of c-Fos (Fig. 2*C*), another AP-1 family member, which does not interact with HBZ (26). Conceivably, HBZ promotes c-Jun degradation without promoting its ubiquitination.

Ubiquitination Is Not Required for HBZ-mediated Proteasomal Degradation of c-Jun—We next determined the role of ubiquitination in HBZ-mediated c-Jun degradation. In the first approach, we constructed a c-Jun mutant (c-JunK/R) in which all lysine residues (potential sites of ubiquitin conjugation) were mutated to arginine. We confirmed that the c-JunK/R mutant was not ubiquitinated in cells (Fig. 3*A*, *left panel*). Wild-type c-Jun and the mutant were confirmed to associate with HBZ comparably (data not shown). As shown in Fig. 3*A* (*right panel*), the c-JunK/R mutant was degraded by HBZ as efficiently as wild-type c-Jun. This result led us to hypothesize that HBZ

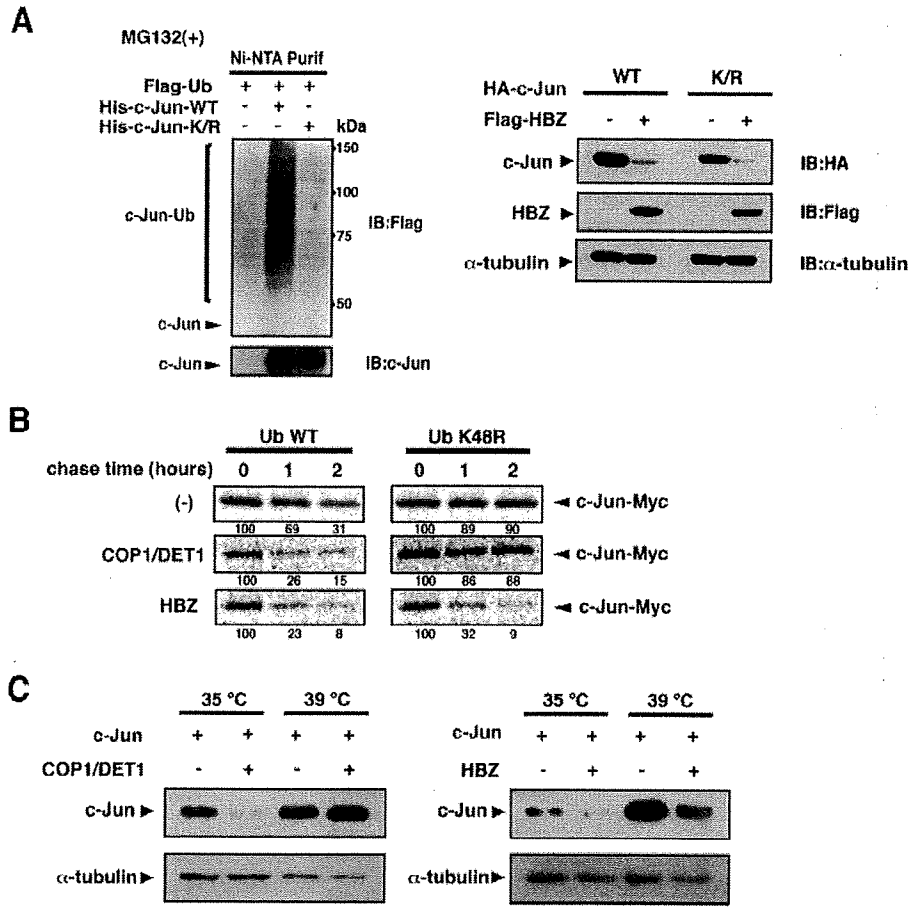

FIGURE 3. **HBZ promotes c-Jun degradation in a ubiquitin-independent manner.** *A*, HBZ promotes the degradation of lysine-free c-Jun. *Left panel*: HEK-293T cells were transfected with 2 μg of either pcDNA3-His-c-Jun or pcDNA3-His-c-JunK/R in the presence of pcDNA3-FLAG-Ub as indicated. After 12 h, the cells were treated with MG132 for 12 h. Following Ni-NTA purification, bound proteins were detected by immunoblot analysis. *Right panel*: HEK-293T cells were transfected with 0.5 μg of either pcDNA3-HA-c-Jun or pcDNA3-HA-c-JunK/R and 3 μg of either pcDNA3 or pcDNA3-FLAG-HBZ. Cell lysates were immunoblotted using the antibodies indicated. *B*, HBZ-mediated degradation of c-Jun is not inhibited by a dominant-negative ubiquitin. HEK-293T cells were transfected with 0.3 μg of pcDNA3-c-Jun-Myc together with 0.5 μg of pcDNA3-HA-COP1 and 1.5 μg of pcDNA3-HA-DET1, or 2 μg of pcDNA3-HA-HBZ in the presence of 3 μg of pcDNA3-FLAG-Ub or -Ub K48R. After 24 h, the cells were pulse-labeled with [^{35}S]methionine/cysteine for 1 h and then chased for the indicated intervals. Labeled c-Jun was immunoprecipitated and resolved by SDS-PAGE. c-Jun levels were detected by autoradiography. The intensity of each band was quantified and listed *below each panel*. *C*, HBZ promotes c-Jun degradation in the absence of a functional ubiquitination system. ts-20 cells were transfected with 1 μg of pcDNA3-FLAG-c-Jun in the presence of 2 μg of pcDNA3-HA-COP1 and pcDNA3-HA-DET1 or 4 μg of pcDNA3-HA-HBZ, as indicated. The cells were then split and incubated at 35 or 39 °C for an additional 24 h. Cell lysates were immunoblotted with anti-FLAG or anti-α-tubulin antibodies.

targets c-Jun for proteasomal degradation in a ubiquitin-independent manner.

In the second approach, we used a dominant-negative ubiquitin mutant (Ub-K48R) that bears a substitution of lysine 48 with arginine. Ub-K48R exerts a chain-terminating effect and blocks ubiquitin-dependent proteasomal degradation (31). In a pulse-chase analysis, the expression of Ub-K48R stabilized c-Jun (Fig. 3*B*, *upper panel*), because c-Jun is basally targeted for ubiquitin-dependent degradation (32). COP1 and DET1, a ubiquitin ligase complex for c-Jun (29), promoted c-Jun degradation in a ubiquitin-dependent manner. Therefore, the expression of Ub-K48R blocked its degradation (Fig. 3*B*, *middle panel*). In contrast, HBZ-mediated degradation of c-Jun was not blocked by Ub-K48R expression (Fig. 3*B*, *lower panel*).

Finally, we performed degradation experiments using the mouse ts20 cell line. These cells have a temperature-sensitive E1 ubiquitin-activating enzyme that is inactivated at the restrictive temperature of 39 °C (33). As expected, ubiquitin-dependent degradation of c-Jun mediated by COP1/DET1 was blocked at 39 °C (Fig. 3*C*, *left panel*), whereas HBZ still promoted c-Jun degradation at the restrictive temperature (Fig. 3*C*, *right panel*). Taken together, these results suggest that HBZ promotes proteasomal degradation of c-Jun through a ubiquitin-independent mechanism.

HBZ Promotes Degradation of Proteins That Bind Its bZIP Domain but Not Its N Terminus—We next examined the specificity of HBZ-mediated proteasomal degradation. In the first approach, we investigated whether HBZ promotes degradation of other bZIP proteins. HBZ has been shown to associate with JunB, JunD, and ATF4 via their bZIP domains (23–25). We found that HBZ also associates with ATF2 through its bZIP domain *in vivo* (Fig. 4*A*, *lower panel*). As shown in Fig. 4*A* (*upper panel*), HBZ promoted degradation of these bZIP-binding proteins, and degradation of these proteins were prevented by MG132 treatment (data not shown). On the other hand, HBZ failed to promote the degradation of CREB and ATF1. Recently, HBZ has been shown to interact with CREB and ATF1 via their bZIP domains *in vivo* and *in vitro* (34). However, we failed to detect these interactions under the experimental conditions in which we readily detected interaction between c-Jun and HBZ (data not shown), likely because these interactions (HBZ-CREB or -ATF1) were very labile or very weak. We previously reported that HBZ does not promote the degradation of c-Fos, a protein that does not interact with HBZ (26). From these results, we predicted a relationship between HBZ association and degradation.

To further investigate this relationship, we constructed a c-Jun mutant lacking the leucine-zipper region (c-JunΔLZ, Fig. 4*B*, *upper panel*) and found that it was unable to associate with HBZ (Fig. 4*B*, *middle panel*). Although HBZ degraded intact c-Jun (Fig. 1), it did not promote degradation of the c-JunΔLZ mutant (Fig. 4*B*, *lower panel*). Furthermore, HBZ did not promote the degradation of p53 (Fig. 4*C*, *lower panel*), which does